MSC-06151
SUPPLEMENT 2

NATIONAL AERONAUTICS AND SPACE ADMINISTRATION

NASA TM-X-70291

APOLLO 15 MISSION REPORT

SUPPLEMENT 2

SERVICE PROPULSION SYSTEM FINAL FLIGHT EVALUATION

MANNED SPACECRAFT CENTER
HOUSTON, TEXAS

NOVEMBER 1972

MSC-05161
Supplement 2

APOLLO 15 MISSION REPORT

Supplement 2

SERVICE PROPULSION SYSTEM FINAL FLIGHT EVALUATION

PREPARED BY

TRW

APPROVED BY

Owen G. Morris
Manager, Apollo Spacecraft Program

NATIONAL AERONAUTICS AND SPACE ADMINISTRATION
MANNED SPACECRAFT CENTER
HOUSTON, TEXAS
November 1972

20029-H102-R0-00

PROJECT TECHNICAL REPORT

APOLLO 15
CSM 112

SERVICE PROPULSION SYSTEM
FINAL FLIGHT EVALUATION

NAS 9-12330

JUNE 1972

Prepared for
NATIONAL AERONAUTICS AND SPACE ADMINISTRATION
MANNED SPACECRAFT CENTER
HOUSTON, TEXAS

Prepared by
R. J. Smith
S. C. Wood
Propulsion Systems Section
Applied Mechanics Department

NASA/MSC

TRW SYSTEMS

Concurred by: _____
Z. D. Kirkland, Head
Systems Analysis Section

Approved by: _____
R. J. Smith, Manager
Task E-99

Concurred by: _____
S. Wood, Manager
Service Propulsion
Subsystem

Approved by: _____
J. M. Richardson, Head
Propulsion Systems
Section

Concurred by: _____
C. W. Yodzis, Chief
Primary Propulsion
Branch

Approved by: _____
R. G. Payne, Manager
Applied Mechanics
Department

TABLE OF CONTENTS

LIST OF TABLES

TABLE OF CONTENTS (Continued)

Page

ILLUSTRATIONS

1. PURPOSE AND SCOPE

The purpose of this report is to present the results of the postflight analysis of the Service Propulsion System (SPS) performance during the Apollo 15 Mission. This report is a supplement to the Apollo 15 Mission Report. The primary objective of the analysis was to determine the steady-state performance of the SPS under the environmental conditions of actual space flight.

This report covers the additional analyses performed following the compilation of Reference 1. The following items are the major additions and changes to the results reported in Reference 1:

1) The steady-state performance as determined from analysis of the third and eighth burns is presented.
2) The analysis techniques, problems and assumptions are discussed.
3) The flight analysis results are compared to the preflight predicted performance.
4) The propellant utilization and gaging system (PUGS) operation is evaluated in greater detail.
5) The pressurization system performance is discussed.
6) The transient data and performance are included.
7) The estimated propellant consumption is revised.

2.0 SUMMARY

Command and service module 112 SPS performance for the Apollo 15 Mission was evaluated and found to be satisfactory. The SPS mission duty cycle consisted of eight firings for a total duration of 590.0 seconds.

SPS steady-stage performance was determined primarily from the analyses of the third lunar orbit insertion and eighth transearth injection burns. It was determined from these analyses that the engine fuel resistance was approximately 7% less than its estimated value based on acceptance test data and post-test reorficing. This compares well within the mean fuel resistance bias of -5.5% determined from postflight analysis of Apollo 9, 10, 11, and 12 (Reference 9) and used in the Apollo 15 preflight analysis, and the -6.7% bias derived from the Apollo 14 Mission postflight analysis.

Average standard inlet condition engine performance values for the two burns analyzed are as follows: thrust, 20846 pounds; specific impusle, 314.7 seconds; and propellant mixture ratio, 1.571. These values are 0.6% greater, 0.1% less, and 0.1% greater, respectively, than corresponding values computed from the preflight engine model, and are within the $\pm 3\sigma$ uncertainties associated with the preflight values.

A systematic oxidizer and fuel propellant tank pressure measurement bias, under engine firing conditions, of approximately -2 psi may have been identified, although further analysis is required to verify that the errors are systematic.

Operation of the Propellant Utilization and Gaging System (PUGS) was satisfactory throughout the mission. The PUGS mode selection switch was set in the normal position for all SPS burns; therefore, only the primary system data were available. By utilizing the propellant utilization valve the crew achieved excellent propellant management with the gageable oxidizer unbalance at the end of the eighth burn being only 25 lbm, decrease.

3.0 INTRODUCTION

The Apollo 15 Mission was the fifteenth in a series of flights using Apollo flight hardware and included the fourth lunar landing of the Apollo Program. The Apollo 15 Mission utilized CSM 112 which was equipped with SPS Engine S/N 65 (Injector S/N 136). The engine configuration and expected performance characteristics (Reference 2) are contained in Table 2. Since previous flight results of the SPS have consistently shown the existence of a negative mixture ratio shift, SPS Engine S/N 65 was re-orificed to increase the mixture ratio for this mission. Figure 22 shows the propellant unbalance for the two major engine firings compared with the predicted unbalance. The unbalance at the end of the transearth injection firing was very small and shows that the modifications to the engine were satisfactory.

The SPS performed eight burns during the mission, with a total burn duration of 590.9 seconds. At approximately 28-2/3 hours after liftoff, the first SPS burn was performed. This was a test burn to verify that the SPS thrust light illumination, which occurred shortly after transposition and docking with the LM, was due to an electrical short existing on the ground side of the SPS pilot valve solenoids. A detailed account of this anomaly may be found in Reference 1. The ignition time, burn duration and velocity gain for each of the eight SPS burns are contained in Table 1.

The electrical short anomaly required a revision to the ignition procedures for the Lunar Orbit Insertion (LOI) and Transearth Injection (TEI) maneuvers. Automatic ignition was accomplished using bank B valves, then bank A valves were opened at ignition plus 5 seconds. Bank A valves

were then manually shut down prior to normal shutdown, thus allowing an automatic shutdown on bank B. The remainder of the maneuvers were accomplished on bank B in the automatic mode.

The first three SPS burns were no-ullage starts, while the remaining burns were preceded by +X Service Module (SM) reaction control system translation maneuvers to ensure SPS propellant settling.

4. STEADY-STATE PERFORMANCE ANALYSIS

Analysis Technique

The major analysis effort for this report was concentrated on determining the steady-state performance of the SPS during the third and eighth burns. The remaining six burns were of insufficient duration to warrant detailed performance analysis. The performance analysis was accomplished with the aid of the Apollo Propulsion Analysis Program (PAP) which utilizes a minimum of variance technique to "best" correlate the available flight and ground test data. The program embodies error models for the various flight and ground test data that are used as inputs, and by statistical and iterative methods arrives at estimations of the system performance history, propellant weights and spacecraft weight which "best" (minimum-variance sense) reconcile the available data.

Analysis Description

The steady-state performance during the third burn was derived from the PAP analysis of a 290-second segment of the burn. The segment analyzed began approximately 40 seconds following ignition. The first 40 seconds of the burn were not included, in order to minimize any errors resulting from data filtering spans which include transient data, and because PUGS data near the start of the burn are not stabilized. The time segment analyzed was terminated approximately 68 seconds prior to SPS shutdown to exclude the three PU valve movements which occurred in the last 68 seconds and to avoid shutdown transients. The burn segment included one PU valve movement, and propellant crossover (storage tank depletion) which occurred about 255 seconds after ignition. The eighth burn steady-state performance was derived from the PAP analysis of a 92 second segment of the

burn. The initial 29 seconds of the burn were excluded from the segment to avoid inclusion of data from the start transient. The burn segment included the PU valve movement which occurred at about 83 seconds from ignition. The segment was terminated approximately 20 seconds prior to engine cutoff in order to exclude shutdown transient data. The steady-state performance analyses of both burns utilized data from the flight measurements listed in Table 3.

The initial estimated spacecraft damp weight (total spacecraft minus SPS propellant) at ignition of the third burn was 62007 lbm. The initial estimated damp weight at ignition of the eighth burn was 24895 lbm. Both values were based on the postflight weight analysis given in Reference 3.

The initial estimates of the SPS propellants onboard at the beginning of the time segment analyzed for the third burn were extrapolated from the loaded propellant weights presented in Section 5. The initial propellant estimates for the time segment analyzed for the eighth burn were extrapolated from the computed propellants remaining at the end of the time segment analyzed for the third burn. All extrapolations of propellant masses used to establish the initial estimates for a given simulation were performed in an iterative manner using derived flowrates and propellant masses from preceding simulations to ensure that the derived propellant mass history was consistent between the two burns analyzed.

The SPS engine thrust chamber throat area was input to the program as a function of time from ignition for each burn. The assumed throat area time history used in the analysis is shown in Figure 1 and was based on the characterization presented in Reference 2.

The SPS propellant densities used in the analysis were calculated from propellant sample specific gravity data obtained from KSC, flight propellant

temperature data, and flight interface pressures. The temperatures used were based on data from feed-system and engine feedline temperature measurements and were input to the program as functions of time. During steady-state operation, it was assumed that respective tank bulk temperatures and engine interface temperatures were equal for both oxidizer and fuel.

The PAP simulations were performed using the "Tank Pressure Driven" SPS model. Simply stated, this model utilizes input oxidizer and fuel tank pressure values, as functions of time, for the starting points in computing the pressures and flowrates throughout the system. The estimated tank pressures input to the program were obtained from a simulation of the complete SPS duty-cycle using the Propulsion Analysis Trajectory Simulation (PATS) program. The PATS program is used to perform the preflight predictions for the SPS. The simulation used to obtain the estimated tank pressures was a "postflight prediction" which used the actual velocity gains for each SPS burn, the actual PU valve position history, the actual bipropellant valve modes, and the postflight reported vehicle weights. The PAP program was free to bias the input tank pressures, if so required, to achieve a minimum variance solution, but was essentially constrained to follow the shape of the input pressures profiles. The shapes of the tank pressure profiles, in turn, strongly influence the computed thrust shape, and therefore, the calculated acceleration shape. The initial simulations of both burns, using the input tank pressure yielded minor computed acceleration shape errors. Analysis of the acceleration shape errors indicated that the input estimated oxidizer and fuel tank pressure shapes were slightly in error. By comparing the interface pressure and acceleration shape errors, it was possible to derive corrections to the input tank pressures which significantly improved the overall data match. The corrections, which were all less than 1.0 psi,

were then input to the program for subsequent simulations.

Analysis Results

The resulting values of the more significant SPS performance parameters, as determined in the analysis, are presented in Tables 4 and 5. Table 4 contains values for the third burn as computed in the PAP simulation. Values are presented for two time slices, which were selected to show performance before and after crossover. Table 5 contains the flight performance values for the eighth burn from the PAP analysis. The values shown are for a representative time slice. In both tables, the corresponding preflight predicted values for the same time slice are also shown. All performance values, both predicted and from the PAP analysis, are at the same PU valve position and should be directly comparable.

Figures 2 and 3 show the calculated SPS specific impulse, propellant mixture ratio, and thrust, as functions of time, for the third burn and the eighth burn, respectively. For comparison the figures also contain the predicted performance. As shown, the specific impulse was between 314.5 and 314.8 seconds throughout both burns. Based on the values computed for the two burns analyzed, and the qualitative comparison of the data from all eight burns, it is concluded that the SPS steady-state performance throughout the entire mission was satisfactory. The propellant mixture ratio agreed well with the predicted at the same PU valve position. It should be noted that the predicted performance for this mission incorporated a mixture ratio bias in order to more closely predict the decreased mixture ratio observed on recent flights. A more detailed comparison of the flight performance to the predicted performance is contained in the following section.

The PAP analysis determined that the best match to the available data required that the engine fuel hydraulic resistance be adjusted from the value used in the preflight analysis (Reference 2). The derived fuel resistance was 894.1 lbf-sec^2/lbm-ft^5. The fuel resistance determined from the engine acceptance tests was 888.1 lbf-sec^2/lbm-ft^5. Based on the acceptance test derived value, the fuel resistance after the post acceptance test reorificing (see Section 2) was estimated to be 962.1 lbf-sec^2/lbm-ft^5. The flight value derived from the analysis was 7.1% less than the estimated reorificed acceptance test value. The flight derived value was only 1.7% less than the value (909.2 lbf-sec^2/lbm-sec^5) used in the preflight prediction. The value used for the prediction was obtained by biasing the estimated reorificed acceptance test value based on postflight experience (Reference 8). An adjustment to the engine oxidizer hydraulic resistance was also required. The flight value derived from the PAP analysis was 473.3 lbf-sec^2/lbm-ft^5, which is 2.2% less than the value derived from acceptance testing and used for the preflight prediction. Because preliminary PAP simulations showed little difference between the resistance values derived from the third burn analyses and those derived from the eighth burn analyses, the final eighth burn simulation was made using the resistances derived from the third analysis.

Significant biases were found to exist in both interface and both propellant tank pressure measurements. The oxidizer interface pressure measurement (SP0901P) data was found to be biased by approximately -4 psi. The fuel interface pressure measurement (SP0930P) data was biased -3 psi. Negative interface pressure biases under flow conditions have been observed on previous flights. Reference 9 contains a statistical analysis of the

interface pressure biases from the Apollo 9 through Apollo 14 Missions. Based on Reference 9, the expected biased were -3.34 psi and -1.54 psi for oxidizer and fuel interface pressure, respectively.

The derived oxidizer(SP0003P) and fuel (SP0006P) propellant tank pressure biases were approximately -2 psi each. The propellant tank pressure measurements are located in the helium supply lines to the tanks and, as such, do not sense tank pressure directly. Examination of the measured tank pressure response at shutdown of the eighth (TEI) burn revealed that immediately (1-5 seconds) following shutdown both pressures rose approximately 2 psi above their respective values prior to shutdown. Considering the relatively fast response of the helium solenoid valves, which are commanded closed at engine cutoff signal, and the large ullage volumes at the end of the eighth burn, the indicated 2 psi rise in tank pressure is totally unreasonable. This gives strong evidence that there was a burn, or flow related, bias on both tank pressure measurements during the firing periods. It is suspected that this bias may be a systematic error associated with transducer location, however, further analysis will be required to verify this possibility and to define the impact, if any, on the preflight prediction model.

The analysis verified that the thrust chamber throat area characterization (Figure 1) was relatively accurate, in that no changes were required to achieve a satisfactory data match for either the third or eighth burn. Both the third and eighth burn PAP analyses indicated that the initial estimates for the spacecraft damp weight were essentially correct with no changes being required.

Early analysis results indicated inconsistencies between the amounts of propellants that were reportedly loaded, the amounts indicated by the

tank gages, and the simulation results. In general, simulations which best matched the sump tank gages after crossover (near the end) of the third burn required either unreasonably large (approximately 130 pounds of oxidizer and 120 pounds of fuel) reductions in the estimated initial propellant masses onboard at the start of the burn segment, or flowrates (and thrust) which did not agree with the storage tank probes and acceleration data. Since the first two burns were of relatively short duration, the propellant loads onboard at the beginning of the third burn should be known to almost the loading tolerances. Furthermore, when the propellants remaining at the end of the third burn for these simulations were extrapolated to the eighth burn, the sump tank probes indicated that the extrapolated quantities (and therefore the computed quantitites remaining at the end of the third burn) were too low by 100-200 pounds for each propellant. Although the extrapolation from the end of the third burn segment to the start of the eighth burn segment was larger (about 150 seconds of total burn time) than in previous postflight analyses, resulting in larger uncertainties in the extrapolations, these discrepancies seemed unreasonable.

The fuel discrepancies were resolved satisfactorily by reducing the fuel onboard at the start of the third burn segment by 50 pounds from the value extrapolated from KSC loading data, and by applying scale factors of 1.0068 and 0.990 to the fuel storage and sump tank gages, respectively. With these corrections, the final simulation gave a fuel mass at the end of the third burn segment which, when extrapolated to the eighth burn, was within 47 pounds of the value determined from the final eighth burn simulation.

The oxidizer discrepancies were similarly resolved by reducing the oxidizer onboard at the start of the third burn segment by 30 pounds from the value extrapolated from the KSC reported load, and by applying a scale factor of 1.0116 and 0.990 to the oxidizer storage and sump tank gages, respectively.

The simulation computed consumption (Table 6) for the whole mission agrees well with consumption from the reported KSC loads and the gaging system readings at shutdown of the eighth burn. Based on the simulation results the total oxidizer and fuel consumed were 23903 and 14984 pounds, respectively. The corresponding values computed from the reported loads and the gage readings (accounting for eighth burn shutdown consumption) were 23913 pounds and 14961 pounds. Based on the computed consumption the overall mission mixture ratio was 1.595, which indicates excellent propellant management. Following the end of the eighth burn, the computed usable[1] oxidizer and fuel quantities remaining were 807 pounds and 484 pounds, respectively. Based on the spacecraft mass at the end of the eighth burn, the estimated SPS ΔV capability remaining was approximately 460 ft/sec[2].

Shown in Figures 4 through 21 are the PAP output plots which present the residuals (differences between the filtered flight data and the program-calculated values) and filtered flight data for the segments of the third and eighth burns analyzed. The figures appear in the following order: vehicle thrust acceleration, oxidizer tank pressure, fuel tank pressure, oxidizer interface pressure, fuel interface pressure, oxidizer sump tank quantity, fuel sump tank quantity, oxidizer and fuel storage tank quantities

(1) Based on unusable quantities of 295.2 pounds and 146.2 pounds of oxidizer and fuel, respectively.

(2) Includes additional allowance of 100 pounds unusable for the ±100 pound PU unbalance meter control ("green") band.

(third burn only), and chamber pressure for the third and eighth burn, respectively. The values for slopes and intercepts seen in the upper right hand corner of these graphs represent the slopes and intercept on the ordinate of a linear fit of the residual data. The closer these numbers are to zero, the better the match.

A strong indication of the validity of the PAP simulation can be obtained by comparing the thrust acceleration calculated in the simulation to that derived from the Apollo Command Module Computer (CMC) ΔV data transmitted via measurement CG001V. This comparison is easily made in terms of the previously mentioned residual slope and intercept data. Figures 4 and 14 show the thrust acceleration during the portions of the burns analyzed, as derived from the CMC data, and the residual between the data and program calculated values. The residual time histories have essentially zero means and little, if any, discernible trend. This indicates that the simulations, especially in terms of the computed specific impulse, are relatively valid, although other factors must also be considered in critiquing the simulations.

As observed on previous flights, the measured chamber pressure drifted with burn time during both burns, presumably because of thermal effects on the transducer. A model of the chamber pressure drift was derived in Reference 9 from a regression analysis of the Apollo 8 through 14 chamber pressure residual errors. The recommended model, which is a fifth degree polynomial in burn time from ignition, was incorporated in PAP and utilized for the first time during this flight analysis. The negligible slopes on the chamber pressure residuals shown in Figures 13 and 21, for the third and eighth burn, respectively, indicate that the drift model successfully accounted for the chamber pressure drift, thereby allowing inclusion of

the chamber pressure measurement data in the analysis. The analysis program results, however, indicated that a large negative (-3 psi) error existed in the measured chamber pressure data for both the burns analyzed. Because the -3 psi error was not observed during the coast periods between burns; i.e. the measured chamber pressure was essentially zero as expected, the error is assumed to be a scale type error as opposed to a fixed bias.

Several of the residual plots for both the third and eighth burns show discontinuities at the times where PU valve movements and propellant crossover occur. These discontinuities are the results of the transients associated with the changes in interface pressure and are not considered significant errors in the match.

Comparison With Preflight Performance Prediction

Prior to the Apollo 15 Mission, the expected performance of the SPS was presented in Reference 2. This performance prediction was for the integrated propellant feed/engine system and, wherever possible, utilized data and characteristics for the specific SPS hardware on this flight.

The predicted steady-state thrust, propellant mixture ratio, and specific impulse are shown in Figures 2 and 3 for the third and eighth burns, respectively. Also shown, for comparison, are the corresponding values for the flight as determined from the steady-state analysis. In general, the comparison of the flight performance to the preflight predicted performance is not straightforward because of the difference in the predicted and actual PU valve position history. The slightly different PU valve position history resulted from the mixture ratio, at a given PU valve position, being somewhat greater than predicted. However, valid comparisons can be made at those times where the predicted and actual PU valve positions are the same.

Previous flight results have consistently shown the inflight mixture ratio to be significantly less than expected based on the engine acceptance test data. As a result, the majority of SPS burn time was performed with the PU valve in the primary increase position. The purpose of the PU valve is to have the capability of adjusting the propellant mixture ratio to 1.60 to 1 (which would ensure a minimum propellant outage). Such mixture ratio shifts, as experienced on previous flights, greatly reduce this capability, and if an even larger shift should occur on future flights this capability would be non-existent. In order to rectify this situation, North American Rockwell directed Aerojet General (Reference 10) to calculate new fuel orifice sizes for Apollo SPS engines S/N 058 and 063 through 072 based on the following conditions:

1) Oxidizer interface orifice to remain unchanged.
2) Engine mixture ratio to be 1.60 to 1.
3) Oxidizer inlet pressure of 162 psia (this is a steady-state flow condition and is unchanged from that value at which the engines were acceptance tested).
4) Fuel inlet pressure of 175 psia (this is also a steady-state flow condition and is increased by 6 psia from that value at which the engines were acceptance tested).

Using the above requirements and the engine acceptance data, the resistan was calculated through the following steps:

1) Using the existing oxidizer resistance, the specified inlet pressures, and the acceptance test value of characteristic exhaust velocity, the chamber pressure calculations were iterated to derive values of oxidizer and fuel flow rates at a mixture ratio of 1.60 to 1 for dual bore.

2) Using the fuel flowrate, the required value of the fuel circuit resistance was calculated. The difference between the existing resistance and the calculated resistance then determined the required increase in the fuel interface orifice.

The reorificed fuel feedline resistance for engine S/N 065 was obtained from the above procedure.

In order to more closely predict the expected inflight mixture ratio based on past flight experience, the reorificed engine fuel hydraulic resistance determined from the acceptance test data was biased by -5.5%. This decreased the mixture ratio expected with the reorificed fuel hydraulic resistances by 2.8% at standard inlet conditions. This bias was obtained by statistically analyzing the results of postflight analyses from Apollo Missions 9, 10, 11, and 12 (Reference 9). The fuel resistance bias derived for the Apollo 14 Mission from the postflight analysis (Reference 11) was -6.7%.

As can be seen in Figures 2 and 3, at common PU valve positions, the flight reconstructed mixture ratio agrees quite well with the predicted mixture ratio. The maximum difference of 0.01 is well within the preflight uncertainty (Reference 2) of ±0.041 (3σ). Similarly, the reconstructed thrust and specific impulse (Figures 2 and 3) were within the prediction uncertainties of ±254 pounds (3σ) and ±1.59 seconds (3σ), respectively, at common PU valve positions.

Engine Performance at Standard Inlet Conditions

The expected flight performance of the SPS engine was based on data obtained during the engine and injector acceptance tests, including data based on the reorificing of the fuel engine feedline (Reference 2). In

order to provide a common basis for comparing engine performance, the acceptance test performance is adjusted to standard inlet conditions. This allows actual engine performance variations to be separated from performance variations which are induced by feed-system, pressurization system, and propellant temperature variations.

The standard inlet conditions thrust, specific impulse and propellant mixture ratio from the engine model used in the preflight prediction are 20716 pounds, 315.1 seconds and 1.570, respectively. Based on the steady-state analysis of the third burn, the standard inlet conditions thrust, specific impulse and propellant mixture ratio were 20850 pounds, 314.8 seconds and 1.571, respectively. These values are 0.65% greater, 0.1% less and 0.11% greater, respectively, than the corresponding values computed from the engine model used in the preflight prediction.

The eighth burn analysis yielded standard inlet conditions thrust, specific impulse and propellant mixture ratio of 20841 pounds, 314.6 seconds and 1.571 units, respectively. These values are 0.60% greater, 0.14% less and 0.11% greater, respectively, than the corresponding values computed from the preflight engine model.

The standard inlet conditions performance values for the two burns agree well with each other, with values for the thrust, specific impulse, and propellant mixture ratio being only 9 pounds, 0.2 seconds, and 0.0 different, respectively. The average standard inlet conditions thrust, specific impulse and propellant mixture ratio for the two burns were 20846 pounds, 314.7 seconds and 1.571 respectively. These values are 0.63% greater, 0.12% less, and 0.11% greater, respectively, than the corresponding values computed from the preflight engine model.

As previously discussed, the engine fuel resistance used in the pre-flight prediction was adjusted from its acceptance test value in an attempt to improve the mixture ratio prediction. If the average standard inlet conditions thrust, specific impulse and mixture ratio from the flight are compared to their corresponding values computed from an engine model based on the unadjusted acceptance test resistances the values are found to be 1.2% greater, 0.1% less and 2.6% less, respectively, than the values from the unadjusted model.

The standard inlet conditions performance values reported herein were calculated for the following conditions.

STANDARD INLET CONDITIONS

Oxidizer Interface Pressure, psia	162
Fuel interface pressure, psia	175
Oxidizer interface temperature, °F	70
Fuel interface temperature, °F	70
Oxidizer density, lbm/ft^3	90.15
Fuel density, lbm/ft^3	56.31
Thrust acceleration, lbf/lbm	1.0
Throat area (initial value), in^2	121.64

Of primary concern in the flight analysis of all Block II engines is the verification of the present methods of extrapolating the specific impulse for the actual flight environment from data obtained during ground acceptance tests at sea level conditions. Since the SPS engine is not altitude tested during the acceptance tests, the expected specific impulse is calculated from the data obtained from the injector sea level acceptance tests using conversion factors determined from Arnold Engineering Developing Center (AEDC) simulated altitude qualification testing. As previously discussed, the average standard inlet conditions specific impulse determined from analyses of the third and eighth burns was 314.7 seconds. The predicted

specific impulse at standard inlet conditions, as extrapolated from the ground test data was 315.1 seconds. The expected tolerance associated with the predicted standard inlet condition value of 315.1 seconds (Reference 2) was ±1.599 seconds (3-σ). The flight value was well within this tolerance. Therefore, it is concluded that the present methods of extrapolating the expected flight specific impulse from the ground test data were satisfactory for this flight, and there is no evidence to warrant changing the methods for future flights. The validity of this conclusion should be continually verified on each subsequent flight.

5. PUGS EVALUATION AND PROPELLANT LOADING

Propellant Loading

The oxidizer tanks were loaded to CM display readout of 100.7% at a tank pressure of 112 psia and an oxidizer temperature of 72.5°F. The fuel tanks were loaded at 110 psia and 68.6°F to a display readout of 100.8%. The SPS propellant loads calculated from these data, and propellant sample density data, are shown in Table 6. As planned, the oxidizer storage tank primary gage was zero adjusted with a nominal -0.4% bias. This zero adjustment bias was incorporated for Apollo 10 and subsequent missions to prevent erroneous storage tank readings after crossover as experienced during the Apollo 9 Mission (Reference 3). The zero adjustment bias causes a small, but known, time varying error (a -0.4% bias and a +0.8% scale factor) in the readings from the storage tank primary gage prior to crossover.

PUGS Operation in Flight

The propellant utilization gaging system (PUGS) operated satisfactorily throughout the mission. The PUGS mode selection switch was set in the normal position for all SPS burns, therefore, only the primary gaging system data were available. The propellant utilization (PU) valve was in the normal position at launch and for the first two burns.

The PU valve was in the normal position for the start of the third burn. Approximately 266 seconds after ignition of the third burn, the PU valve moved to the decrease position. At about 339 seconds from ignition the PU valve was returned to the normal position and left there for about five seconds. At about 344 seconds from ignition the PU valve was moved to the decrease position. The PU valve remained in decrease until about 383 seconds from ignition, at which time the PU valve was returned

to the normal position. The PU valve was in the normal position for the remainder of the third burn, and all of the fourth, fifth, sixth and seventh burns, and for approximately the first 83 seconds of the eighth burn, at which time it was moved to the decrease position. The PU valve was left in the decrease position for the remainder (approximately 58 seconds) of the eighth burn.

Figure 22 shows the indicated propellant unbalance history for the third and eighth burns; as computed from the filtered T/M PUGS data. The indicated unbalance history should reflect the CM display unbalance history, within the T/M accuracy. The actual indicated unbalance at the end of the eighth burn was 20 pounds, increase, which agrees reasonably well with the crew reported unbalance reading of 25 pounds, decrease. The expected unbalance and associated PU valve position history, which are also shown in Figure 22, are seen to differ only slightly with the actual. As expected, based on past flights, the indicated unbalance following the start of the third burn showed decrease readings. The initial decrease readings are cuased by three factors: 1) the previously mentioned -0.4% calibration bias on the oxidizer storage tank probe, 2) ungageable oxidizer (approximately 100 pounds) above the top of the oxidizer sump tank probe prior to crossover due to propellant transfer resulting from helium absorption, and 3) the tendency of the fuel probes to read erroneously high for about 30-40 seconds following ignition of low acceleration burns due to capillary action in the probe stillwells. The first two error sources are accounted for in the preflight model, resulting in the initial 115 pound decrease reading shown (Figure 22) for the expected unbalance. Because the third error source (the erroneously high fuel probe readings near the ignition transient)

caused errors of relatively short duration, and because the planned crew logic calls for no PU valve movements in the initial portion (first 20-30 seconds) of the burn, no attempt was made to account for this phenomenon in the preflight model. After propellant crossover, at about 240 seconds into the third burn, the unbalance is seen to take a step increase as the effects of the two known oxidizer sump tank gaging errors (the -0.4% bias and the oxidizer above the sump tank probe) are eliminated. Throughout the balance of the third burn (after 285 seconds) and during the eighth burn the unbalance was satisfactorily controlled within the ±100 lbm unbalance "green band" by the use of the PU valve. At the end of the eighth burn the unbalance was reported by the crew as only 25 pounds, decrease.

6.0 PRESSURIZATION SYSTEM EVALUATION

Operation of the helium pressurization system was satisfactory without any indication of leakage. The helium supply pressures indicated nominal helium usage for the eight SPS burns.

The propellant tanks were pressurized several days prior to launch, and at liftoff the measured tank pressures were approximately 179 psia for the oxidizer and 182 psia for the fuel.

During the launch phase and coast period to the first SPS burn, the measured oxidizer and fuel tank pressures decayed, as expected, to approximately 168 psia and 174 psia, respectively, due primarily to helium absorption into the propellants.

This mission was the second to utilize the SPS engine to perform the descent orbit insertion maneuver. The very precise ΔV requirements for this burn made any over or underburn highly undesirable, and, therefore, a crew timed backup cutoff was implemented. Because of the critical nature of this burn an analysis was performed (Reference 2) to determine the best estimate for the propellant tank pressure rises from the end of the LOI burn time, are dependent on the initial tank pressures. Such propellant tank pressure increases have been experienced on past Apollo flights and are attributed to propellant vapor resaturation and temperature recovery of the ullage which occur following a long burn in which there is a significant percentage increase in ullage volume. The predicted pressure rises were 6.7 psia (from 176.5 psia) for the oxidizer tank and 3.6 psia (from 176.8 psia) for the fuel tank, and the pressure rises experienced on Apollo 15 were 7 psia (from 177 psia) for the oxidizer tank and 4.5 psia (from 177.5 psia) for the fuel tank.

The GN_2 actuation system pressures indicated satisfactory usage. At launch the storage pressures for GN_2 Systems A and B were both approximately 2495 psia. Following the eighth and final SPS burn the T/M data indicated that the System A pressure was 2295 psia and that the System B pressure was 2095 psia. System A was utilized on three SPS burns for an indicated average pressure decrease of approximately 67 psia per burn. System B was utilized on eight burns for an indicated average pressure decrease of 50 psia per burn.

7. ENGINE TRANSIENT ANALYSIS

A summary of the start and shutdown transient performance data for all SPS firings, except for the fifth firing, is presented in Table 7. The start impulse for both the fourth and sixth burns exceeded the upper specification limit of 700 lbf-sec by 14 lbf-sec. The difference between the seventh burn and the fourth, sixth and eighth burns exceeded the start impulse run-to-run specification limits of ±200 lbf-sec. Because of the measurement uncertainty associated with the chamber pressure data used to compute impulse, the out-of-specification values are not considered significant. The start times(ignition to 90 percent of steady-state thrust) for each burn were all within the specification limits. The computed shutdown impulse for all burns was well within the specification limit of 10,000 lbf-sec, and the variability between burns was within the ±500 lbf-sec specification limits, with the exception of the fourth and eighth burns. The shutdown time (cutoff to 10 percent of steady-state thrust) for each burn were all within specification limits.

Because the first and second burns were of such short duration (less than 1 second) the total vacuum impulse from ignition to shutdown (10% steady-state thrust) was computed for these burns. The specification values for these burns were obtained from the Spacecraft Operational Data Book (Reference 2), and correspond to the expected total vacuum impulse for burns of such duration.

The electrical short anomaly (Section 3.0) required a revision to the ignition procedures for the Lunar Orbit Insertion (LOI) and Transearth Injection (TEI) maneuvers. Automatic ignition was accomplished using bank B valves, then bank A valves were opened at ignition plus 5 seconds. Bank

A valves were then manually closed prior to normal shutdown, thus allowing an automatic shutdown on bank B. The remainder of the maneuvers were accomplished on bank B in the automatic mode. There were no detrimental effects from the revised procedures.

The chamber pressure overshoot values are contained in Table 7 and were all within the specification limit of 120 percent.

8.0 REFERENCES

1. NASA Report MSC-05161, "Apollo 15 Mission Report," December 1971.

2. Spacecraft Operational Data Book, SNA-8-D-027, Vol. I, Part 1, Amendment 67, 25 May 1971.

3. TRW IOC 71.6522.2-03, "Apollo 15 Postflight Mass Properties," C. A. Anderson, 23 September 1971.

4. TRW Technical Report 11176-H311-R0-00, "Apollo 9 CSM 104 Service Propulsion System Final Flight Evaluation," 4 August 1969.

5. TRW Technical Report 11176-H526-R0-00, "Apollo 10 CSM 106 Service Propulsion System Final Flight Evaluation," 31 March 1970.

6. TRW Technical Report 17618-H019-R0-00, "Apollo 11 CSM 107 Service Propulsion System Final Flight Evaluation," September 1970.

7. TRW Technical Report 17618-H058-R0-00, "Apollo 12 CSM 108 Service Propulsion System Final Flight Evaluation," November 1970.

8. TRW Technical Report 17618-H129-R0-00, "Apollo Primary Propulsion System Engineering Mathematical Models," March 1971.

9. TRW IOC 71.4915.2-61, "Service Propulsion System (SPS) Characterization," 25 October 1971.

10. Aerojet General CEM 380, "New Fuel Interface Orifices for Apollo SPS Engines 058, 063 through 072," received MSC 4 January 1971.

11. TRW Techanical Report 17618-H214-R0-00, "Apollo 14 CSM 110 Service Propulsion System Final Flight Evaluation," September 1971.

TABLE 1

APOLLO 15 SPS DUTY CYCLE

MANEUVER	FS1 (G.E.T.)	FS2 (G.E.T.)	BURN DURATION (SEC)	VELOCITY CHANGE (FT/SEC)
TEST	28:40:22.00	28:40:22.80	0.80	5.5
MCC-4	73:31:14.81	73:31:15.72	0.91	5.4
LOI	78:31:46.70	78:38:25.06	398.36	3000.1
DOI	82:39:49.09	82:40:13.62	24.53	213.9
CIRC	101:38:58.98	101:39:02.65	3.67	68.3
LOPC	165:11:32.74	165:11:51.05	18.31	330.6
SHAPE	221:20:48.02	221.20:51.44	3.42	66.4
TEI	223:48:45.84	223:51:06.74	140.90	3046.8
			590.90	6737.0

TABLE 2

CSM 112 SPS ENGINE AND FEED SYSTEM CHARACTERISTICS

Engine No.	65
Injector No.	136
Chamber No.	348
Initial Chamber Throat Area (in^2)	121.6403

Engine and System Fluid Resistances ($lbf\text{-}sec^2/lbm\text{-}ft^5$)

	Based on Acceptance Test	Based on Reorificing	Adjusted
Fuel Engine Feedline	888.1	962.1	909.2
Oxidizer Engine Feedline	482.7		
Fuel System Feedline	36.08		
Oxidizer System Feedline			
PU Valve in Pri-normal position	97.72		
PU Valve in Pri-increase	48.43		
PU Valve in Pri-decrease position	165.26		

Characterization Equation for C*:

$$C^* = C^*_{S.C.} + 870.5\,(MR - 1.6) - 273.83\,(MR^2 - 2.56) - 0.31878\,(P_C - 99) + 12.953\,(TP - 70) - 0.07414\,(TP^2 - 4900) - 5.466\,(MR \cdot TP - 112) + 0.03119\,(MR \cdot TP^2 - 7840.);$$

where $C^*_{S.C.}$ (Engine No. 65) = 5998.9 ft/sec

Characterization Equation for Isp:

$$I_{SP} = I_{SP_{vac}} - 96.954\,(1.6 - MR) - 0.0487\,(99 - P_C) - 0.06276\,(70 - TP) + 30.409\,(2.56 - MR^2) + 0.0004483\,(4900 - TP^2);$$

where $I_{SP_{vac}}$ (Engine No. 65) = 315.0 lbf-sec/lbm

TABLE 3

FLIGHT DATA USED IN STEADY-STATE ANALYSIS

Measurement Number	Description	Range	Sample Rate Samples/Sec
SP0930 P	Pressure, Engine Fuel Interface	0 to 300 psia	10
SP0931 P	Pressure, Engine Oxidizer Interface	0 to 300 psia	10
SP0661 P	Pressure, Engine Chamber	0 to 150 psia	100
SP0003 P	Pressure, Oxidizer Tanks	0 to 250 psia	10
SP0006 P	Pressure, Fuel Tanks	0 to 250 pisa	10
SP0048 T	Temperature, Engine Fuel Feed Line	0 to 200 °F	1
SP0049 T	Temperature, Engine Oxidizer Feed Line	0 to 200 °F	1
SP0056 T	Temperature, 1 Fuel Distribution Line	0 to 200 °F	1
SP0655 Q	Quantity, Oxidizer Tank 1 Primary - Total Auxiliary	0 to 50%	1
SP0656 Q	Quantity, Oxidizer Tank 2	0 to 60%	1
SP0657 Q	Quantity, Fuel Tank 1 Primary - Total Auxiliary	0 to 50%	1
SP0658 Q	Quantity, Fuel Tank 2	0 to 60%	1
CG0001 V	Computer Digital Data	40 Bits	1/2

TABLE 4

APOLLO 15

SERVICE PROPULSION SYSTEM STEADY-STATE PERFORMANCE

THIRD SPS BURN

(LOI)

PARAMETER	INSTRUMENTED					
	Before Crossover FS-1 + 100 sec.			After Crossover FS-1 + 265 sec.		
	Predicted	PAP	Measured	Predicted	PAP	Measured
PU Valve Position	Normal	Normal	Normal	Normal	Normal	Normal
Oxidizer Tank Pressure, Psia	175	177	175	176	177	176
Fuel Tank Pressure, Psia	176	176	174	177	177	176
Ox Interface Pressure, Psia	162	162	159	165	166	162
Fuel Interface Pressure, Psia	172	173	170	175	175	173
Engine Chamber Pressure, Psia	101	101	100	102	103	102
	DERIVED					
Oxidizer Flowrate, lbm/sec	40.4	40.9	--	41.1	41.6	--
Fuel Flowrate, lbm/sec	25.2	25.4	--	25.4	25.6	--
Propellant Mixture Ratio	1.602	1.611	--	1.616	1.625	--
Vacuum Specific Impulse, Sec	315.1	314.8	--	315.2	314.8	--
Vacuum Thrust, lbf	20654	20841	--	20950	21133	--

Notes:
(1) Predicted values from Reference 2.
(2) Calculated values from Propulsion Analysis Program
(3) Measured data are as recorded and are not corrected for biases and errors discussed in text.

TABLE 5

APOLLO 15

SERVICE PROPULSION SYSTEM STEADY-STATE PERFORMANCE

EIGHTH SPS BURN

(TEI)

PARAMETER	INSTRUMENTED		
	FS-1 + 89 Sec.		
	Predicted	PAP	Measured
PU Valve Position	Decrease	Decrease	Decrease
Oxidizer Tank Pressure, Psia	178	179	177
Fuel Tank Pressure, Psia	177	177	175
Oxidizer Interface Pressure, Psia	159	160	155
Fuel Interface Pressure, Psia	175	175	172
Engine Chamber Pressure, Psia	101	101	101
DERIVED			
Oxidizer Flowrate, lbm/sec	39.5	39.8	--
Fuel Flowrate, lbm/sec	25.8	25.8	--
Propellant Mixture Ratio	1.535	1.542	--
Vacuum Specific Impulse, sec	315.0	314.6	--
Vacuum Thrust, lbf	20561	20658	--

Notes:

(1) Predicted values from Reference 2
(2) Calculated values from Pronulsion Analysis Program
(3) Measured data are as recorded and are not corrected for biases and errors discussed in text.

TABLE 6
APOLLO 15
SPS PROPELLANT DATA

Propellant	Total Mass Loaded (lbm) Computed From Loading Data	Based on Analysis
Oxidizer	25035.6	2500.52
Fuel	15664.0	15614.3
TOTAL	40699.6	40619.5

Propellant	Propellant Consumption (lbm) Computed From Loading Data and PUGS[1]	Analysis Results
Oxidizer	23912.6	23903.2
Fuel	14961.0	14984.3
TOTAL	38873.6	38887.5

Propellant	Propellant Residuals (lbm) Computed From PUGS[1]	Analysis Results
Usable Oxidizer	828	807
Usable Fuel	557	484
TOTAL	1385	1291

(1) Crew reported command module computer panel readings

TABLE 7
APOLLO 15
ENGINE TRANSIENT DATA

PARAMETER	SPECIFICATION VALUE		APOLLO 15 SPS MANEUVERS						
	Single Bore	Dual Bore	1st	2nd	3rd	4th	6th	7th	8th
Total Vacuum Impulse (Ignition to 90% Steady-State Thrust), lbf-sec	450 ±250 (a) ±200 (b)	568			592	714	714	423	657
Time (Ignition to 90% Steady-State Thrust), sec	0.675 ±0.100				.667	.652	.711	.699	.715
Chamber Pressure Overshoot, Percent	120		113	107	113	111	111	109	107
Total Vacuum Impulse (cutoff to 0% steady-state thrust), lbf-sec	12,500 ± 2,500 (a) ± 500 (b)	13,500 ± 2,500 (a) ± 500 (b)			12,979	12,343	13,076	12,595	13,281
Time (Cutoff to 10% Steady-State Thrust), sec	1.075	1.075			1.061	1.025	1.052	1.017	1.104
Minimum Impulse Burn, Total Vacuum impulse, lbf-sec	18,000 (c) 16,000 (d)		16,160	16,666					
Time (FS1 to FS2), sec			0.80	0.91					

(a) Engine-to-Engine Tolerance
(b) Run-to-Run Tolerance
(c) Nominal impulse value for a burn of 0.91 seconds duration.
(d) Nominal impulse value for a burn of 0.80 seconds duration.

Note: All maneuvers had single bore starts and shutdowns.

FIGURE

SPS CHAMBER THROAT AREA

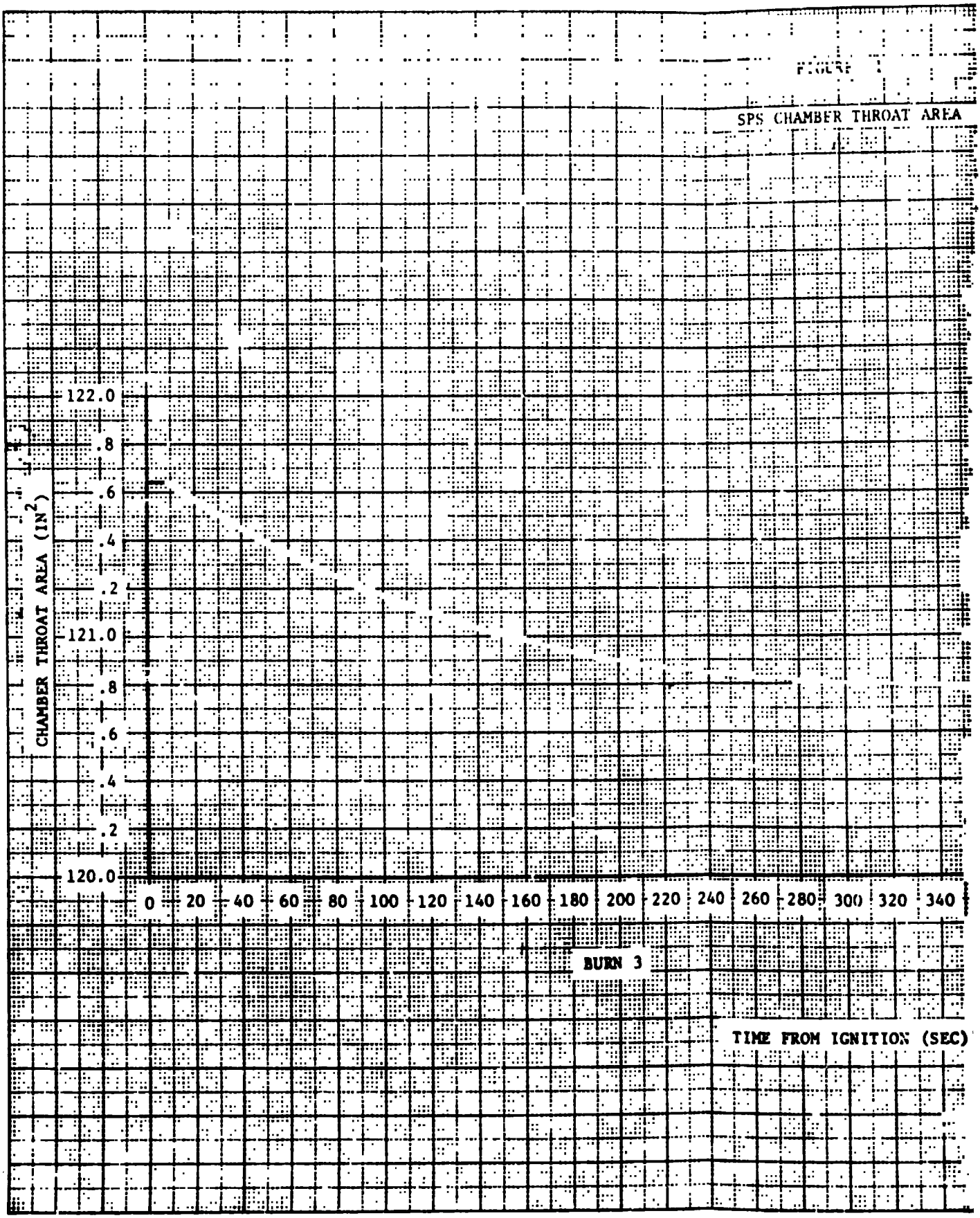

FOLDOUT FRAME

FC

FIGURE 1

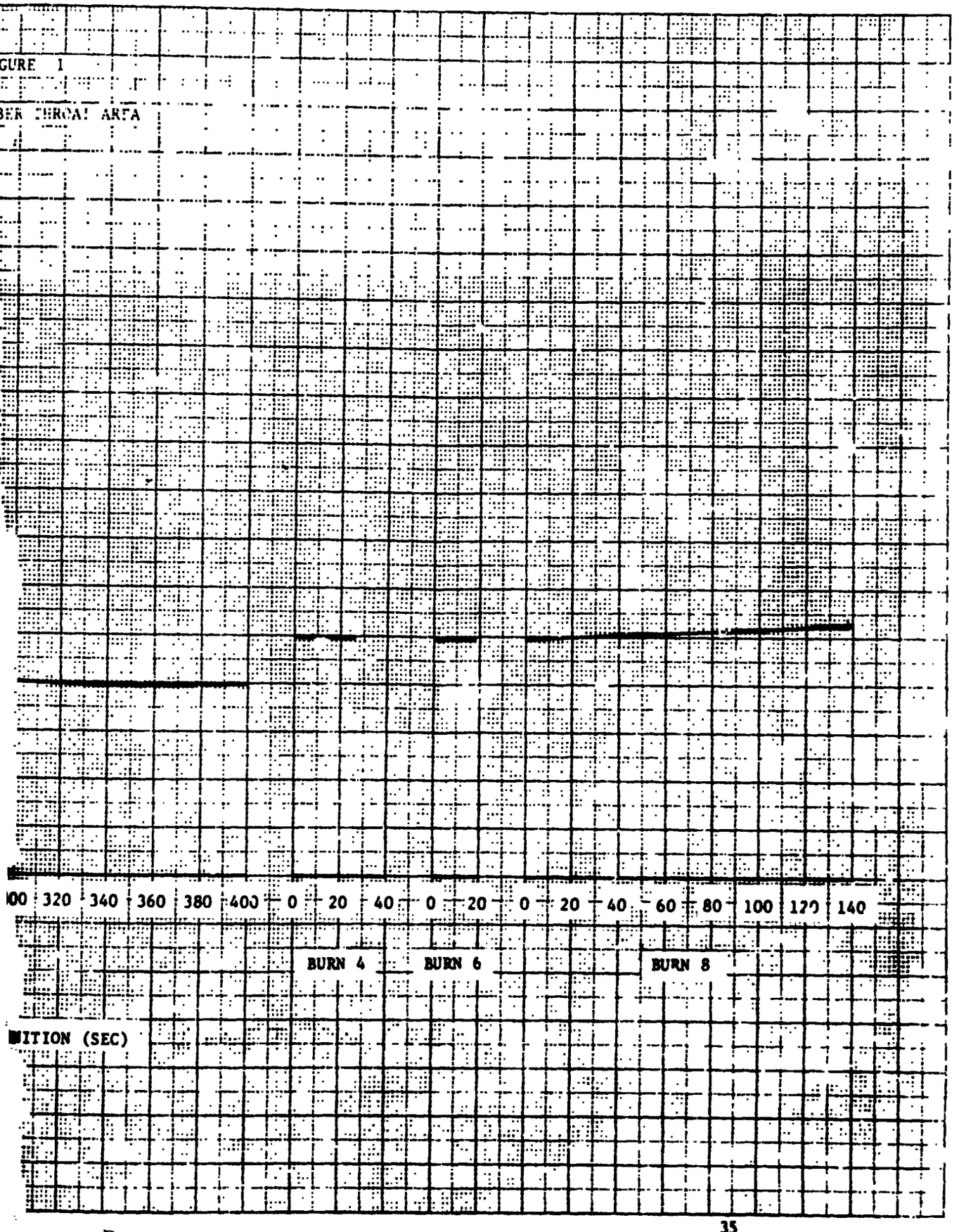

FOLDOUT FRAME 2

FIGURE 2

APOLLO 15

COMPARISON OF PREDICTED AND INFLIGHT PERFORMANCE (THIRD BURN) (LOI)

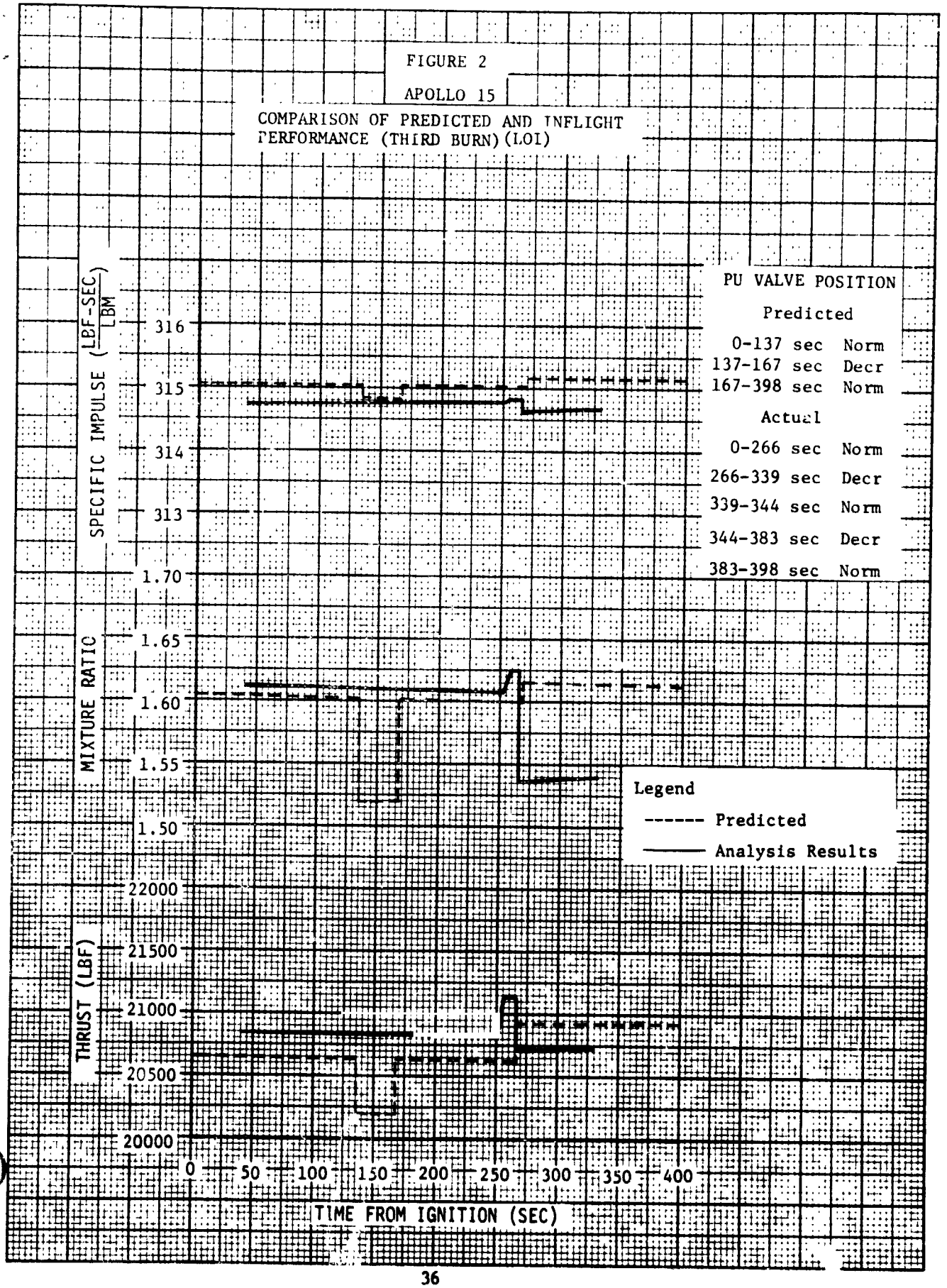

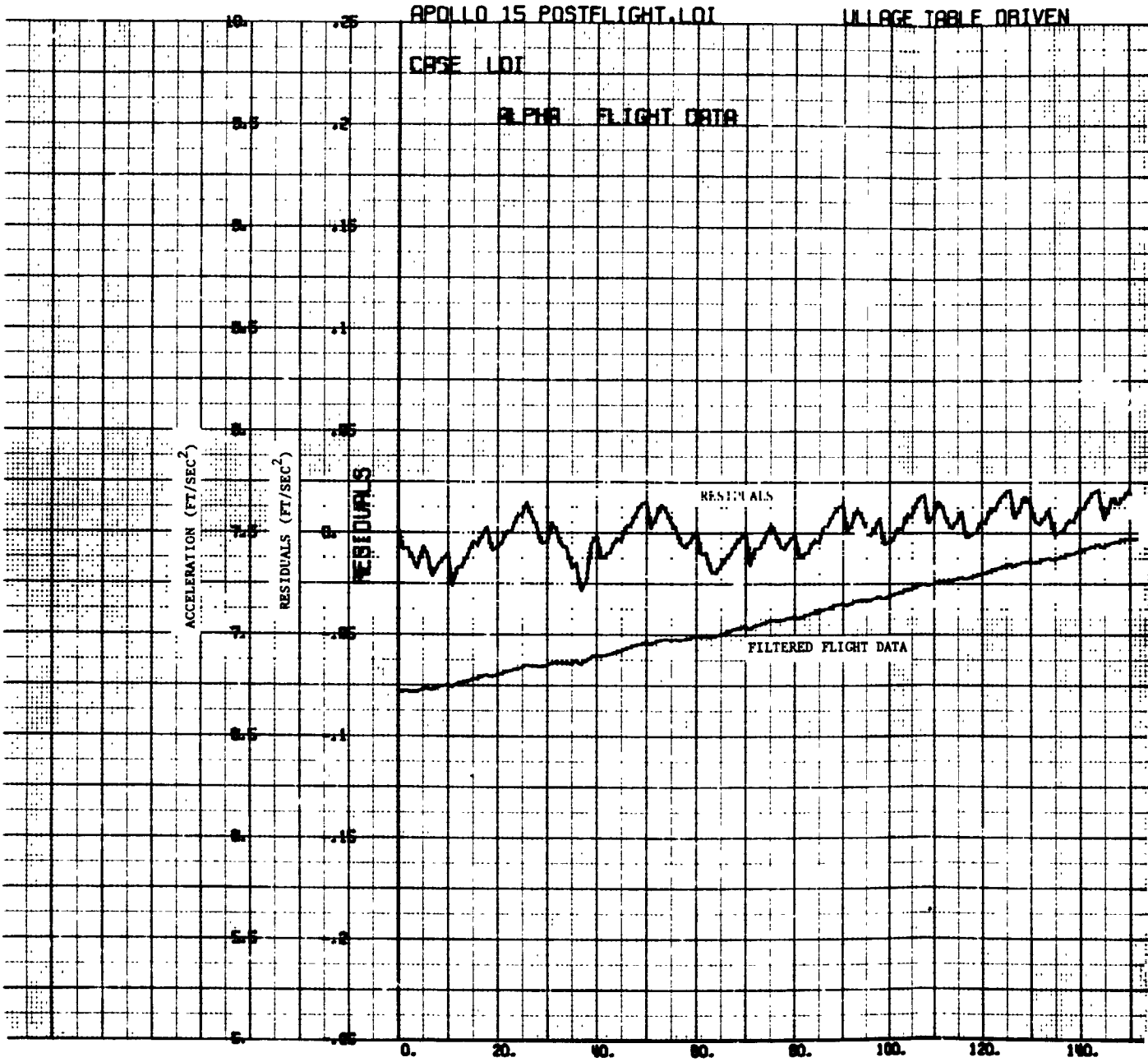

FOLDOUT FRAME

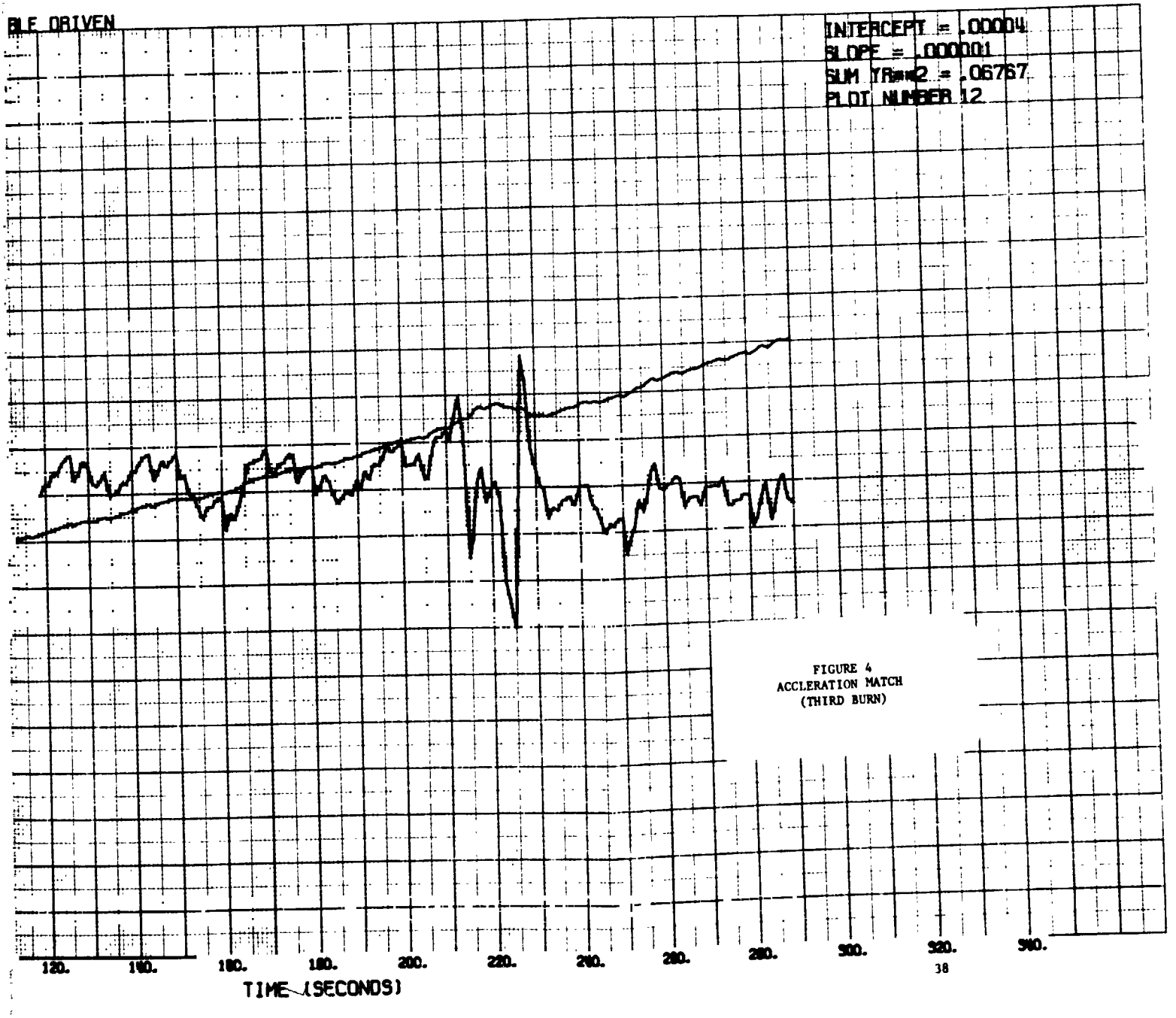

FIGURE 4
ACCLERATION MATCH
(THIRD BURN)

FOLDOUT FRAME

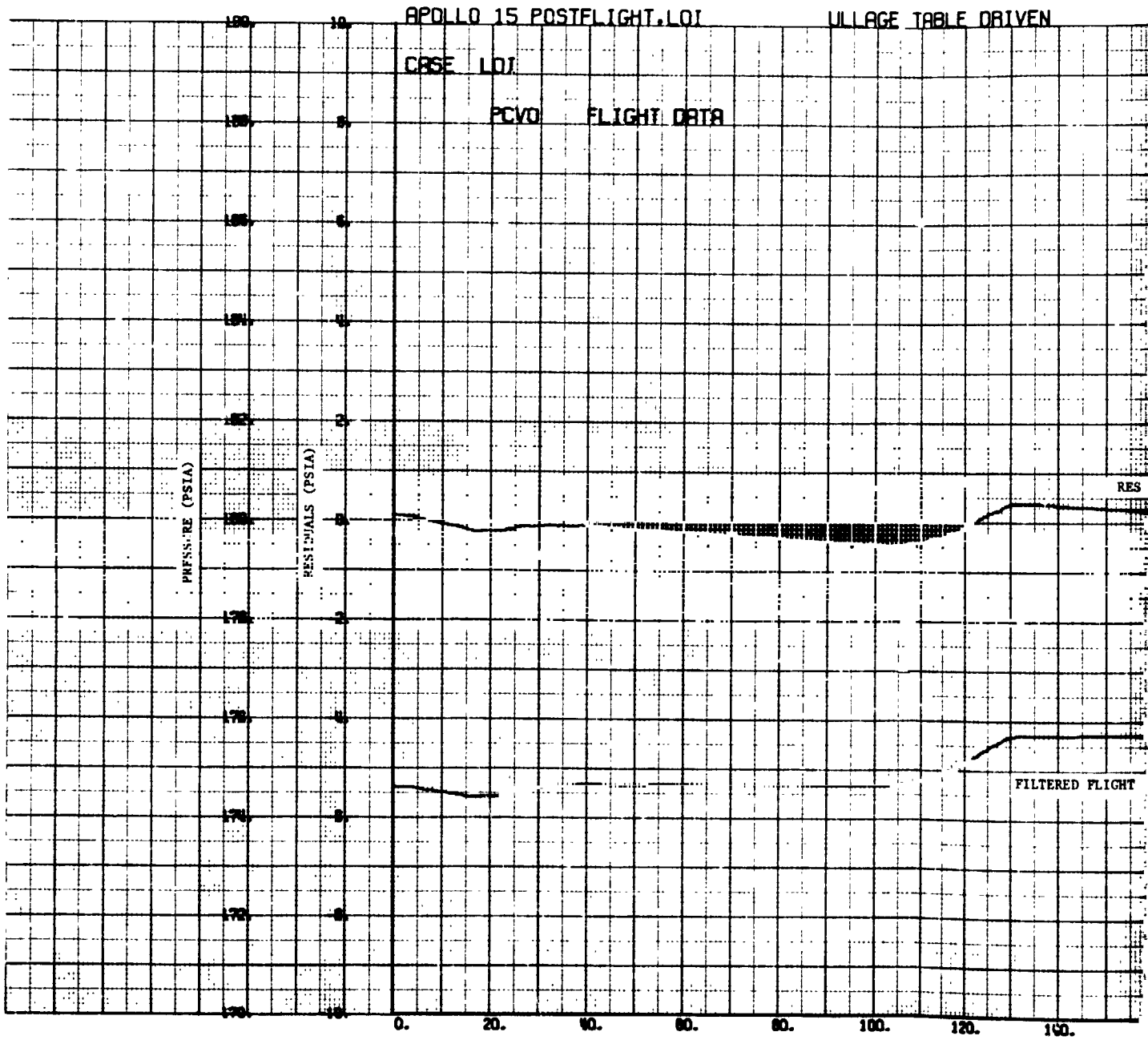

FOLDOUT FRAME

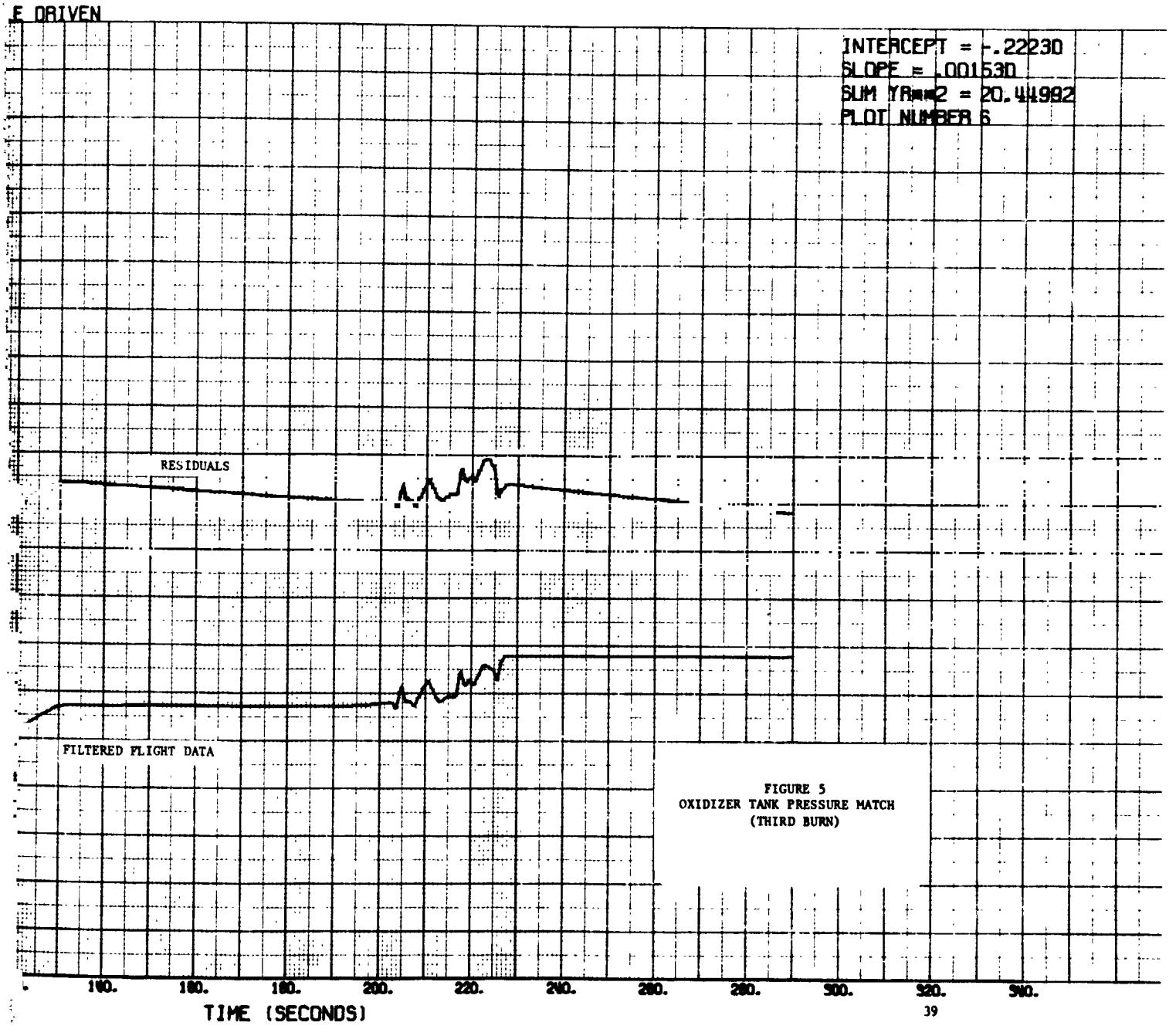

FIGURE 5
OXIDIZER TANK PRESSURE MATCH
(THIRD BURN)

Previous Card

2

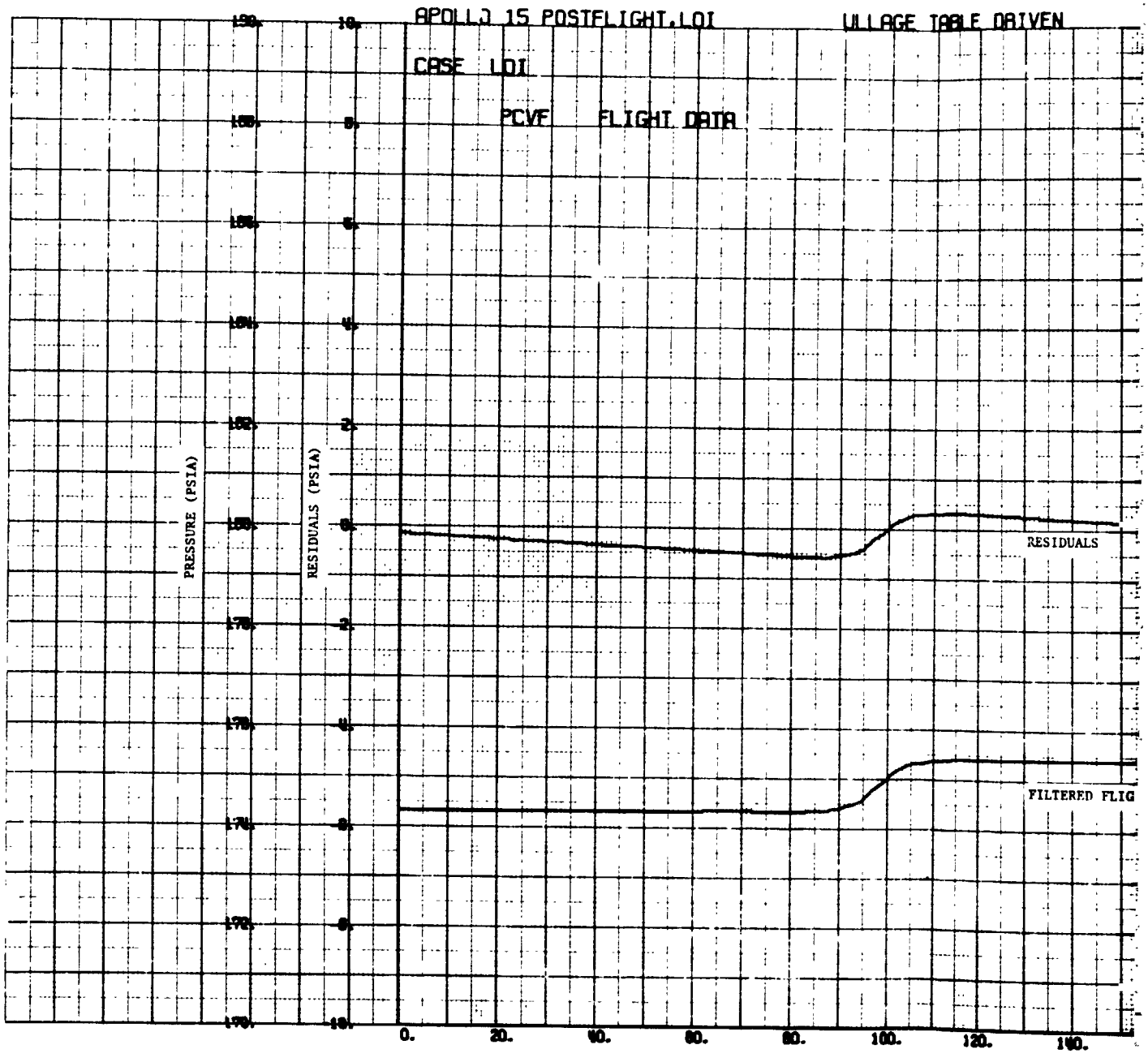

FOLDOUT FRAME

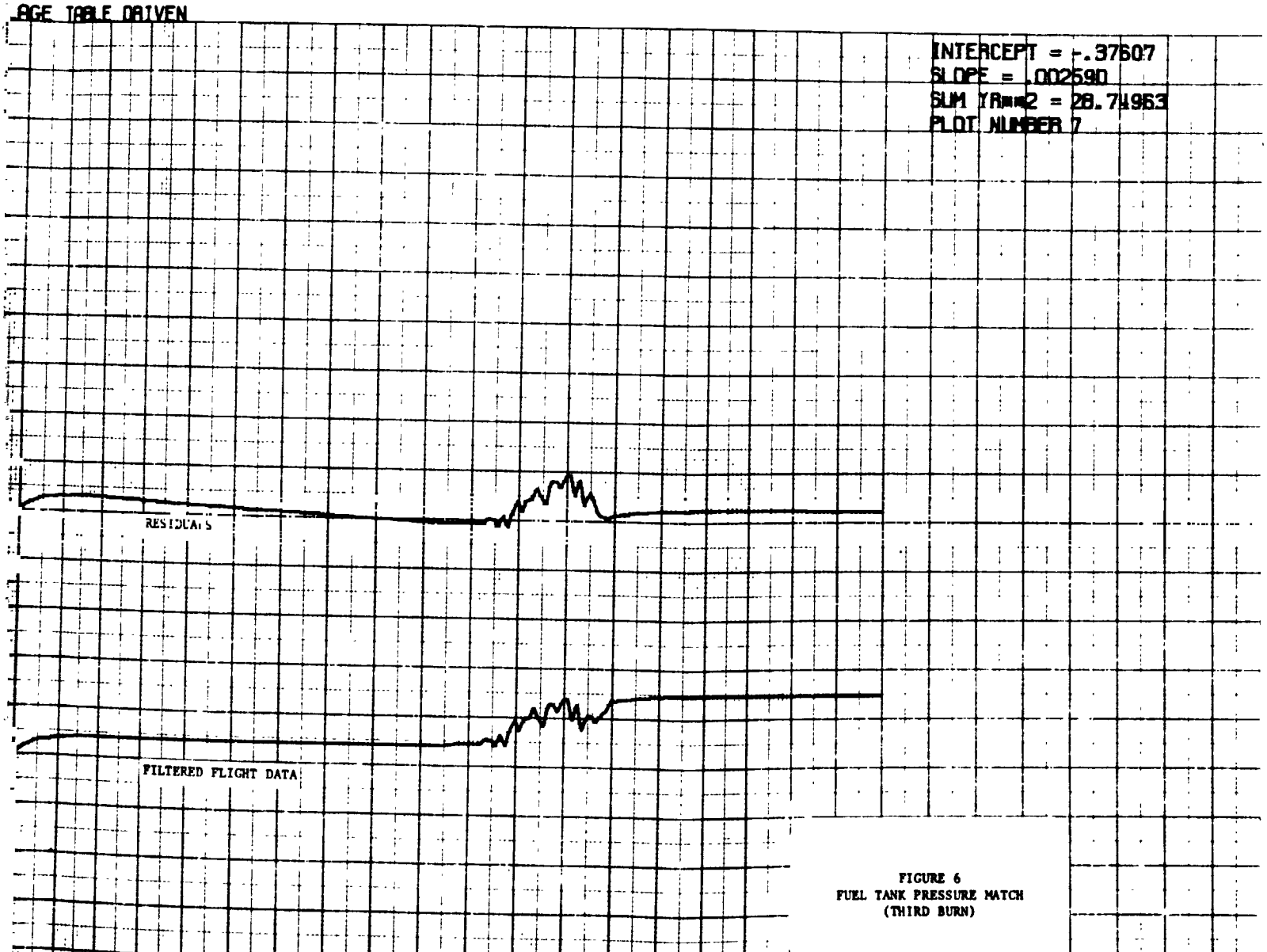

FIGURE 6
FUEL TANK PRESSURE MATCH
(THIRD BURN)

FOLDOUT FRAME

2

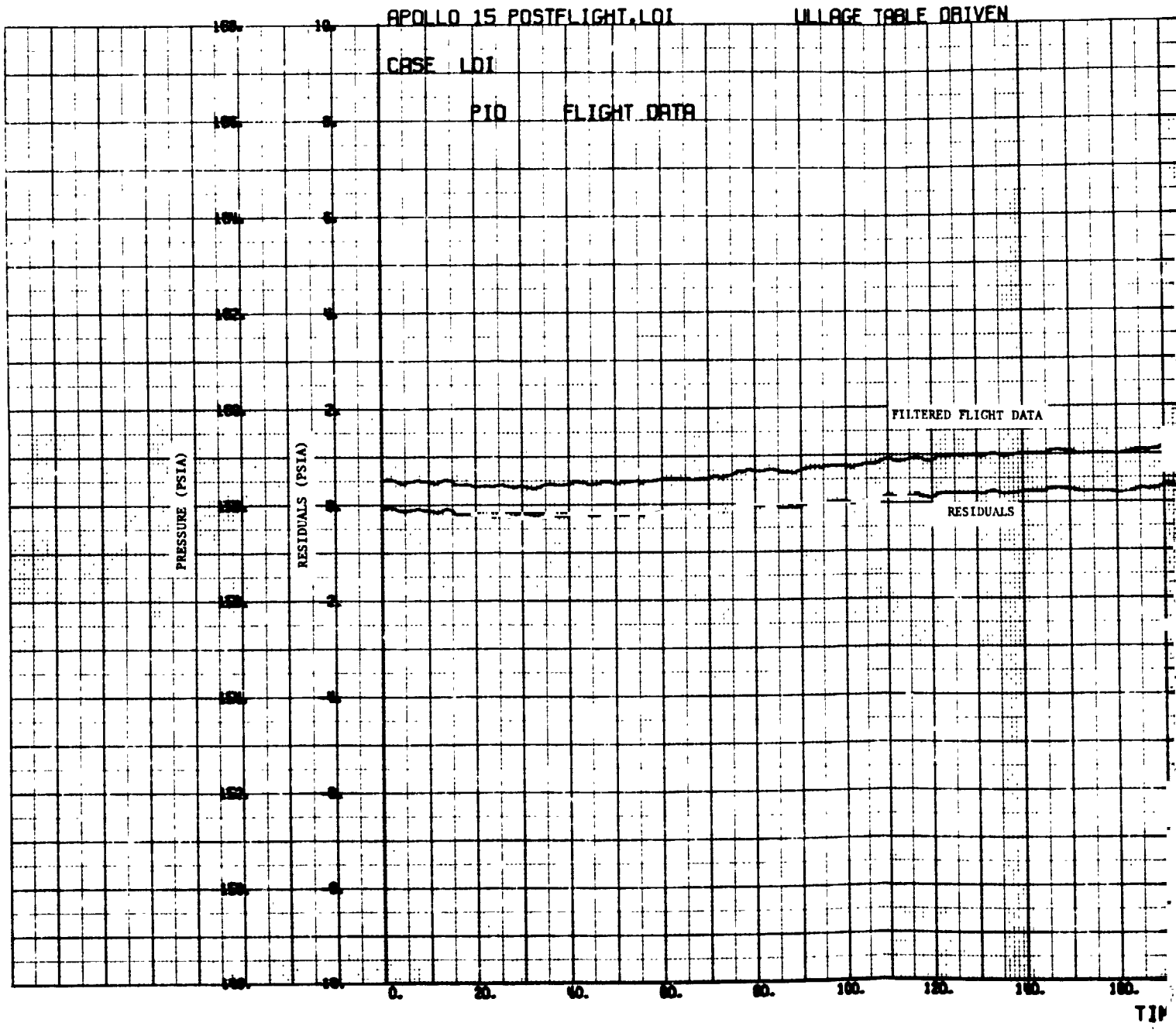

FOLDOUT FRAME

1

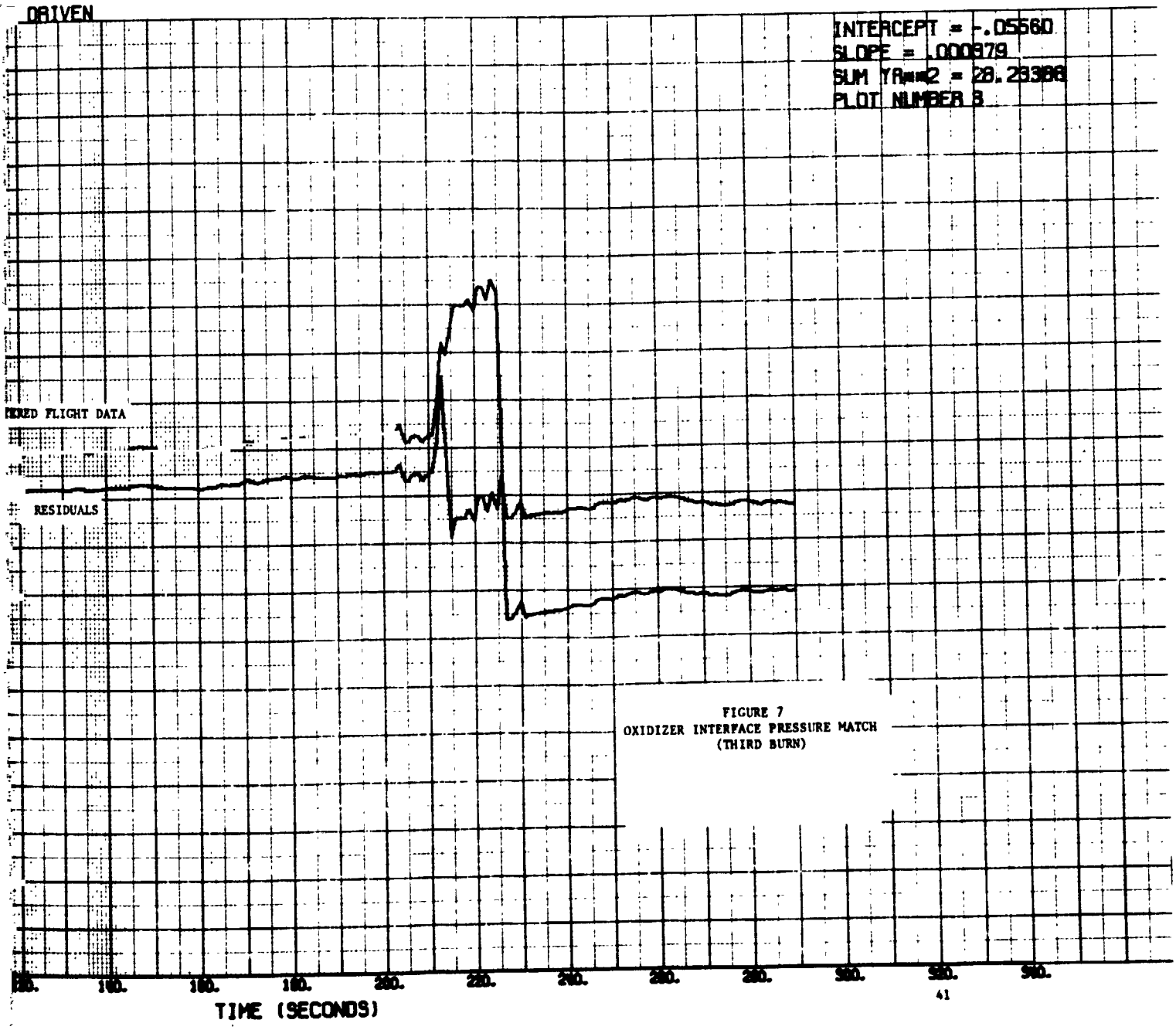

FIGURE 7
OXIDIZER INTERFACE PRESSURE MATCH
(THIRD BURN)

FOLDOUT FRAME

2

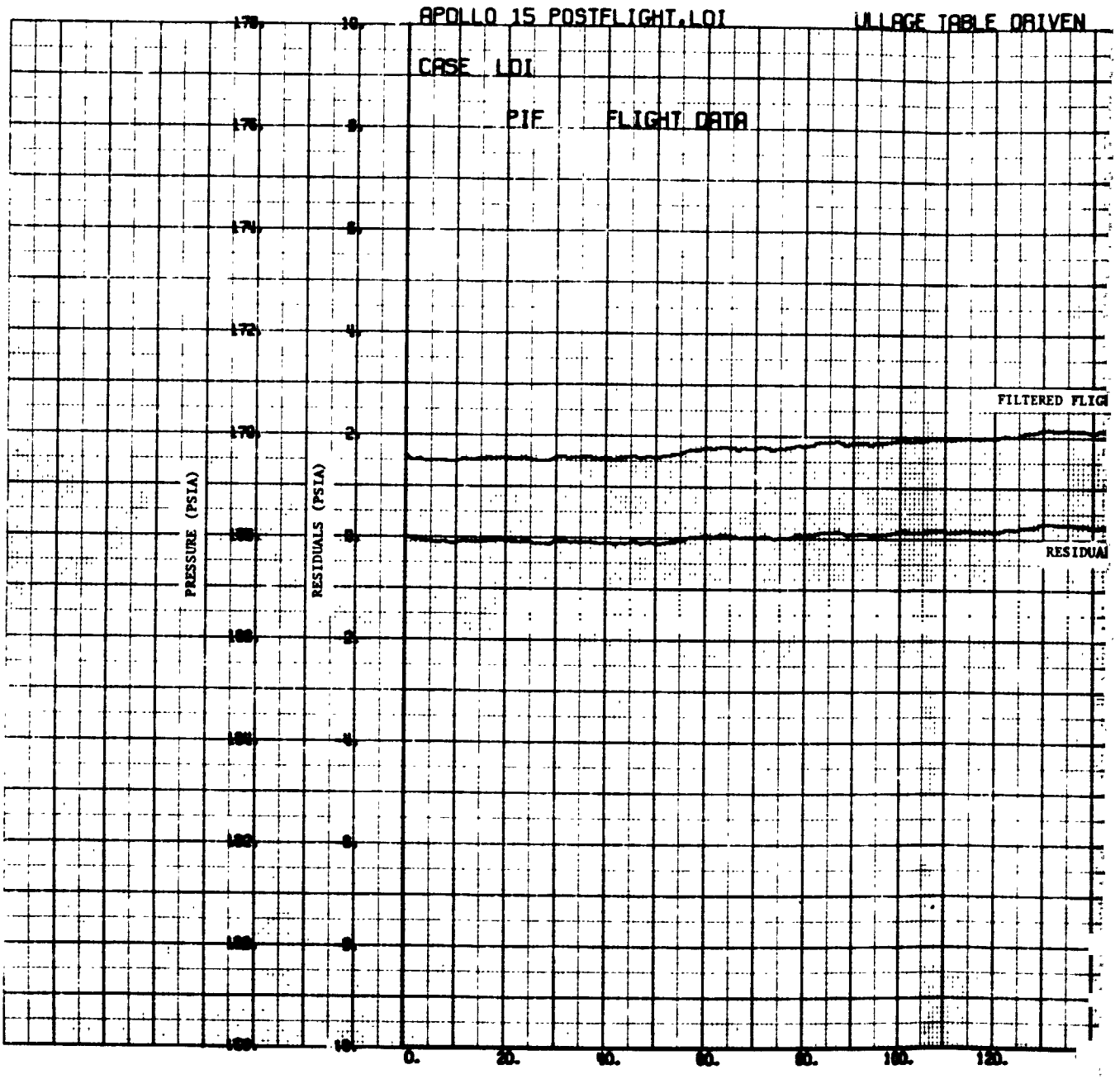

FOLDOUT FRAME

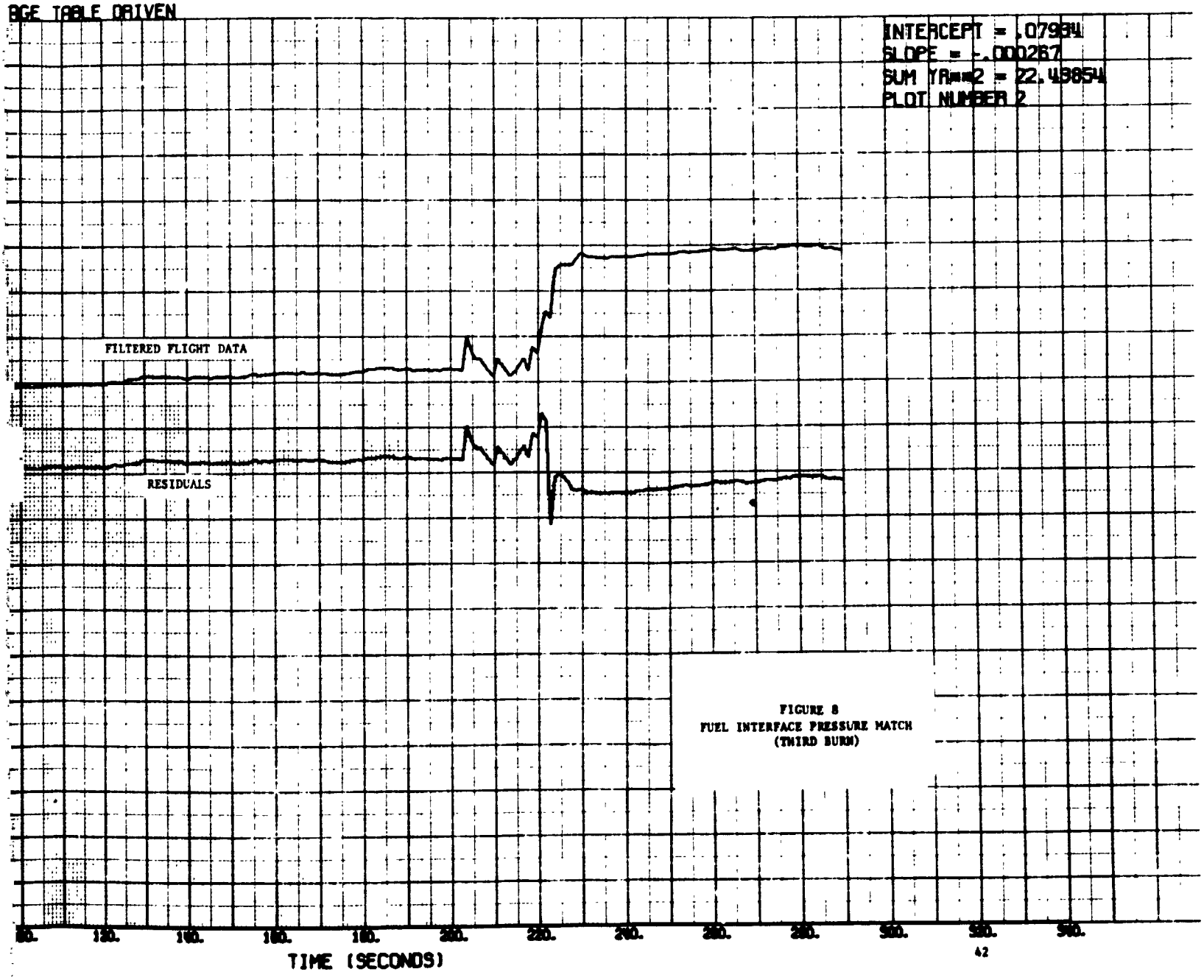

FIGURE 8
FUEL INTERFACE PRESSURE MATCH
(THIRD BURN)

FOLDOUT FRAME

2

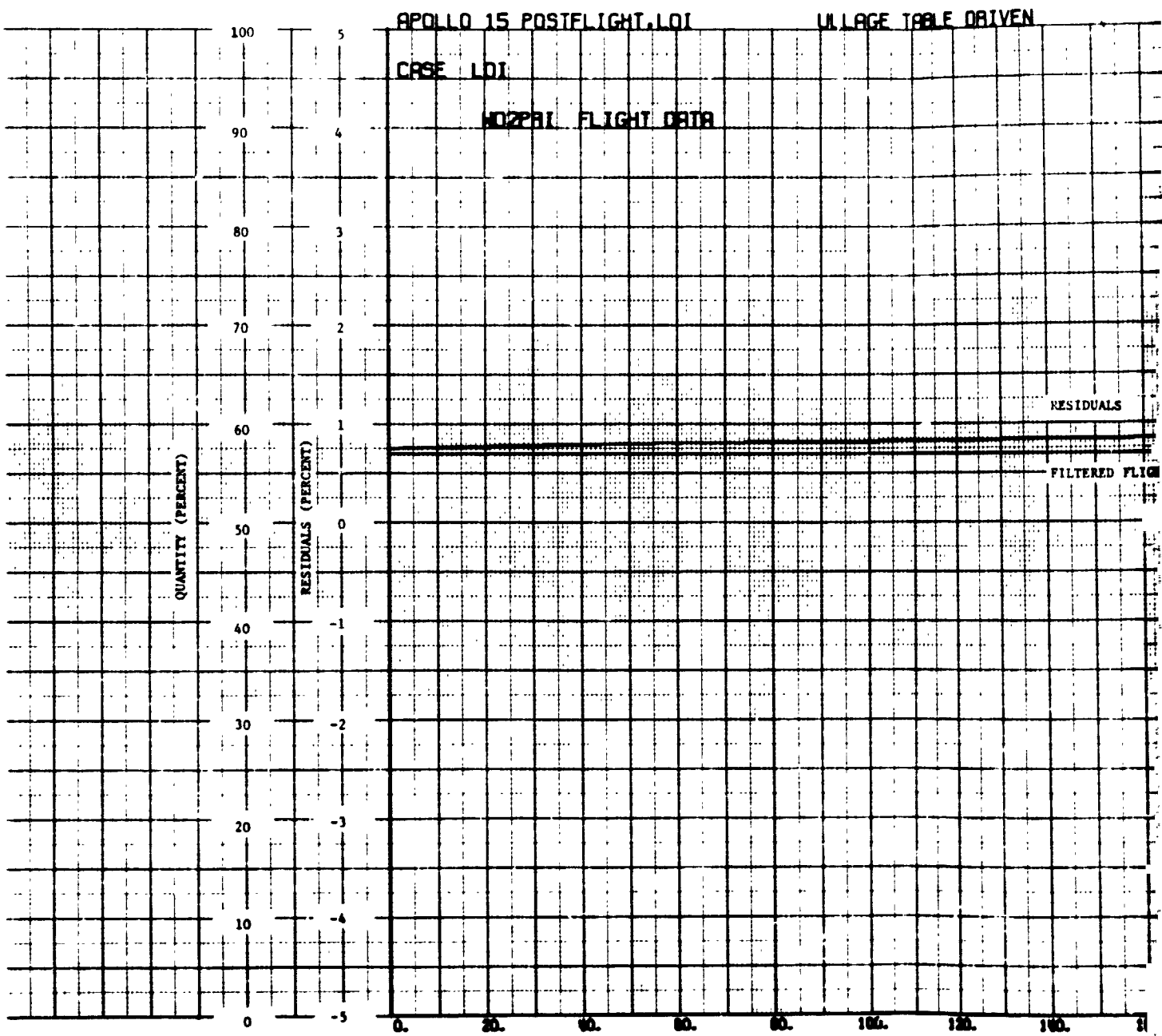

FULLOUT FRAME

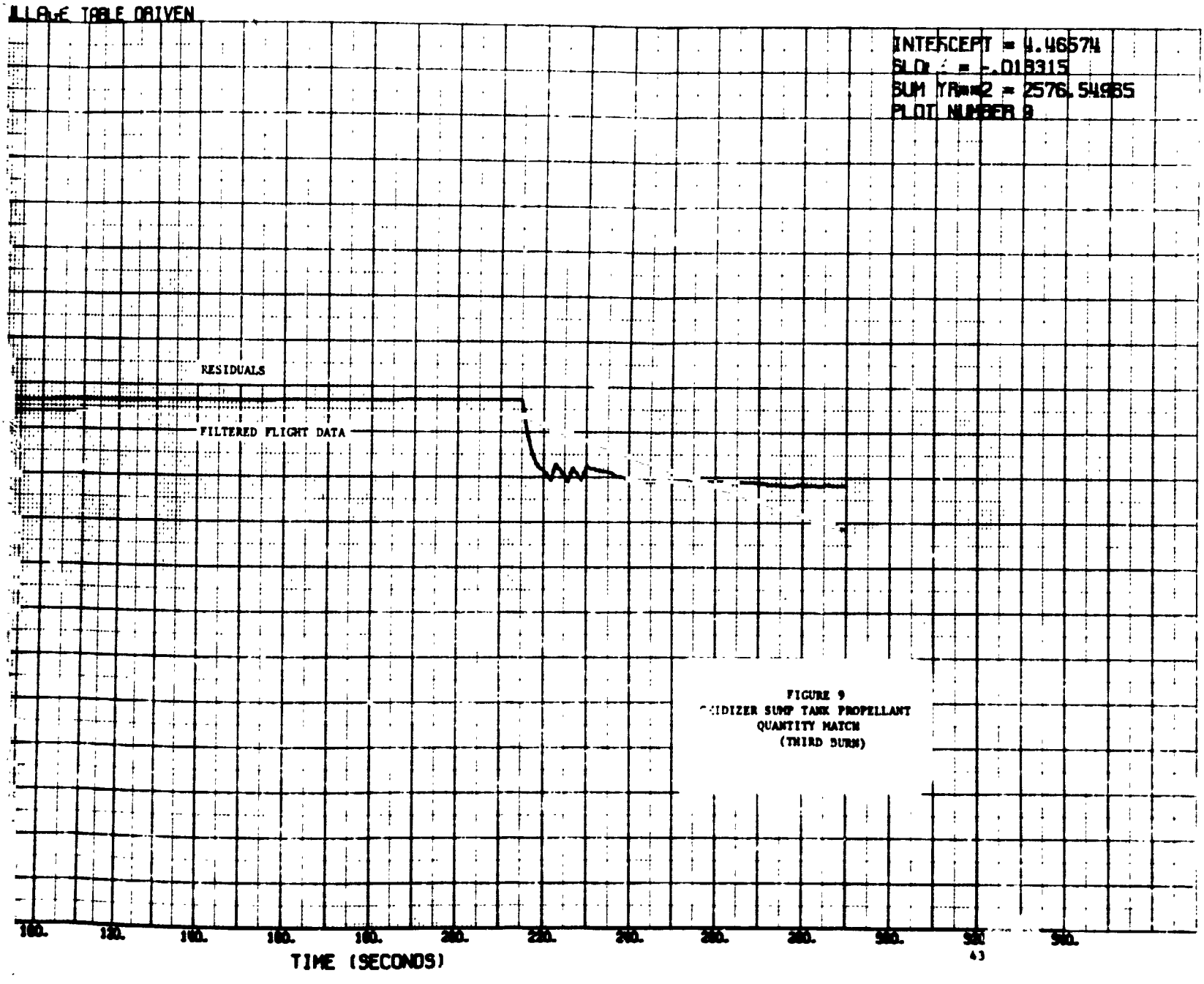

FIGURE 9
OXIDIZER SUMP TANK PROPELLANT
QUANTITY MATCH
(THIRD BURN)

FOLDOUT FRAME

2

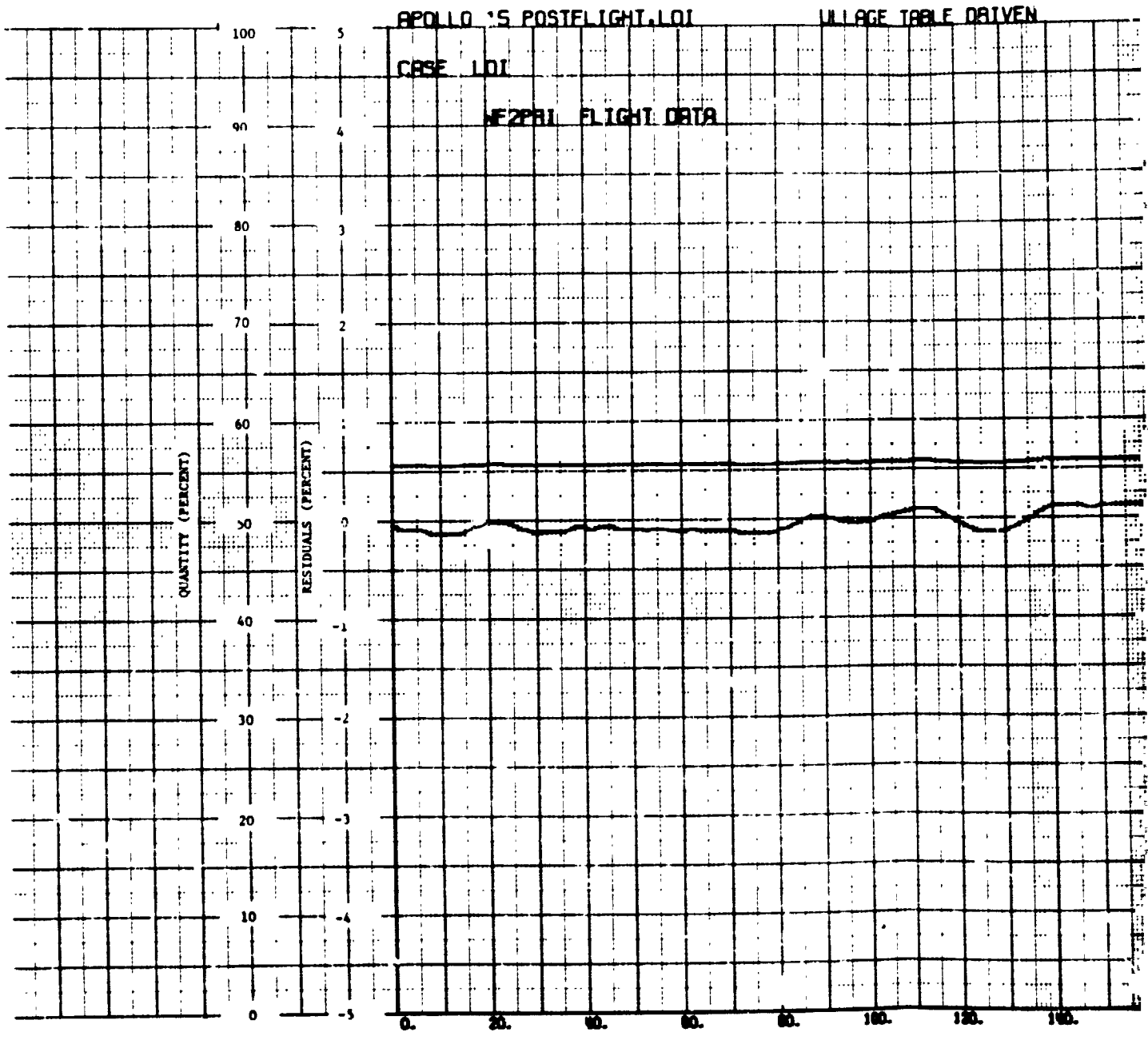

FOLDOUT FRAME

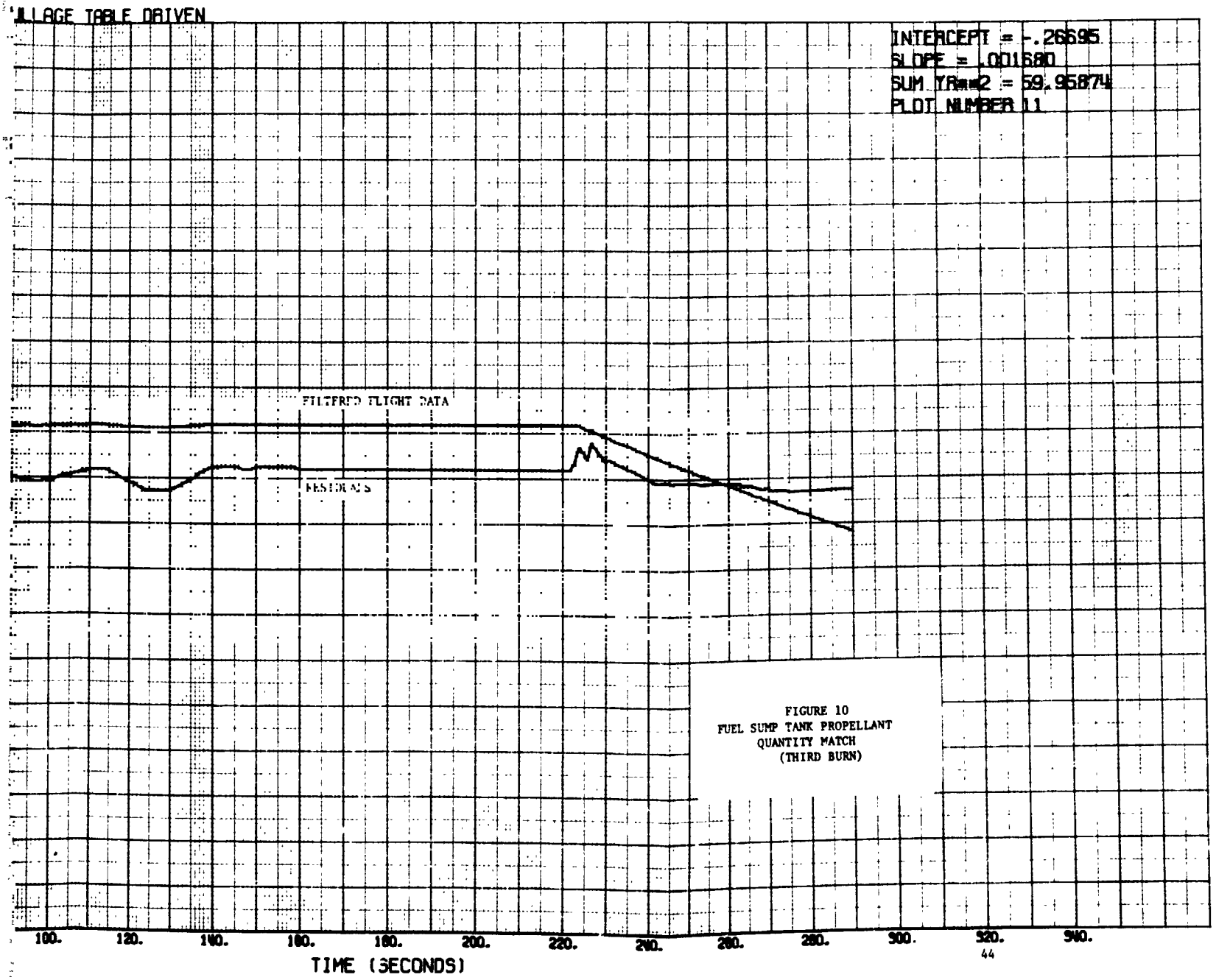

FIGURE 10
FUEL SUMP TANK PROPELLANT
QUANTITY MATCH
(THIRD BURN)

FOLDOUT FRAME

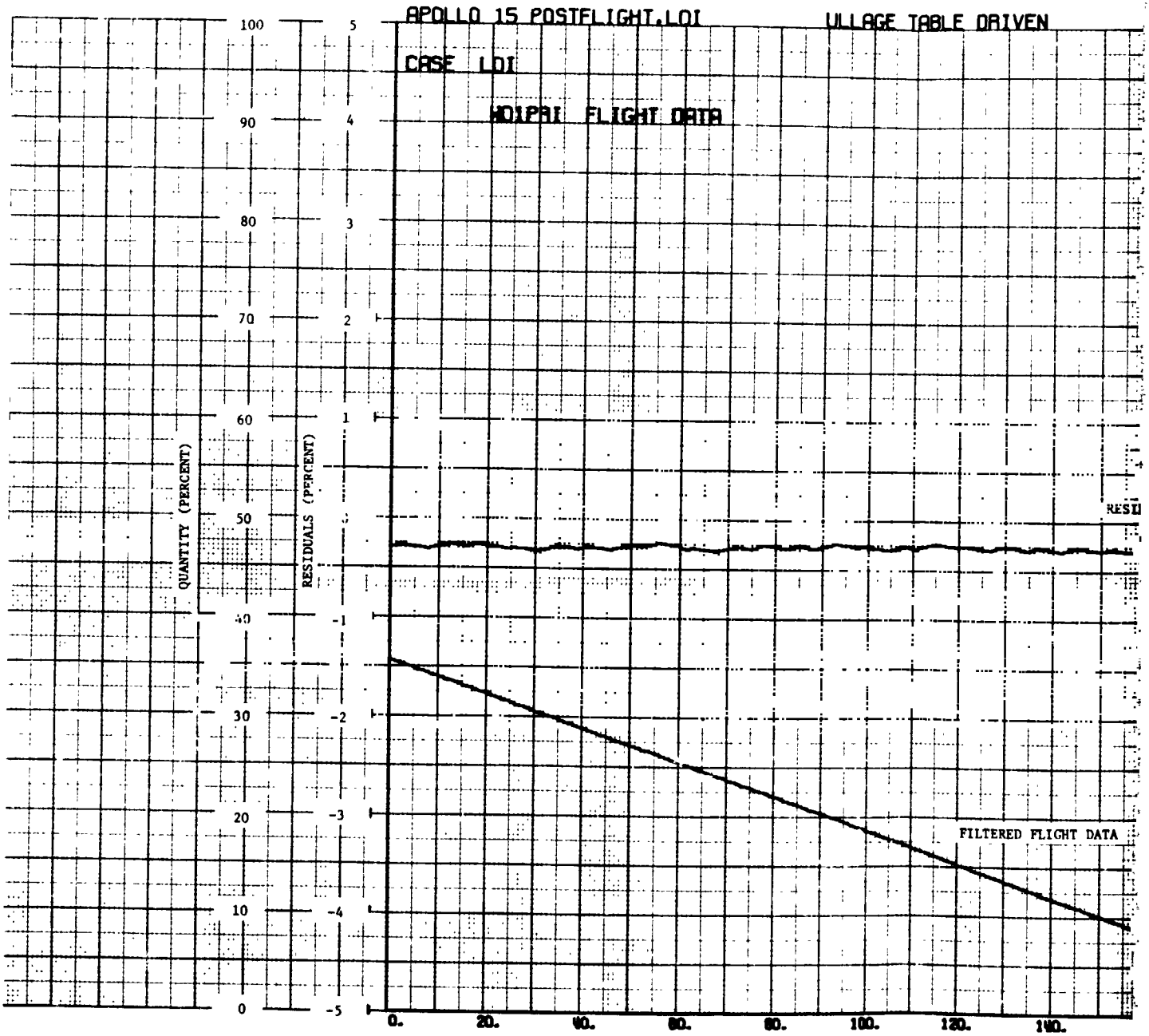

FOLDOUT FRAME

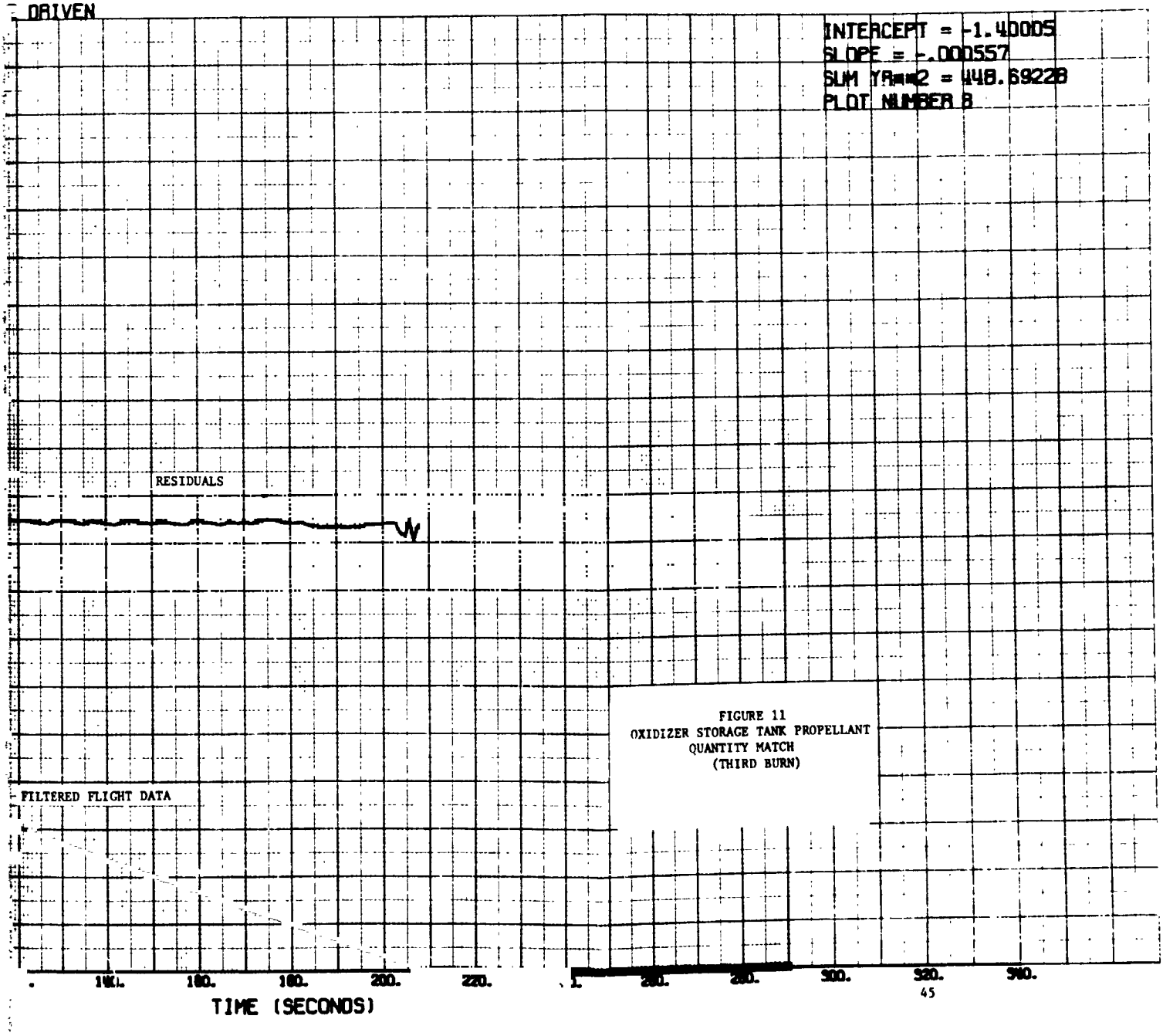

FIGURE 11
OXIDIZER STORAGE TANK PROPELLANT
QUANTITY MATCH
(THIRD BURN)

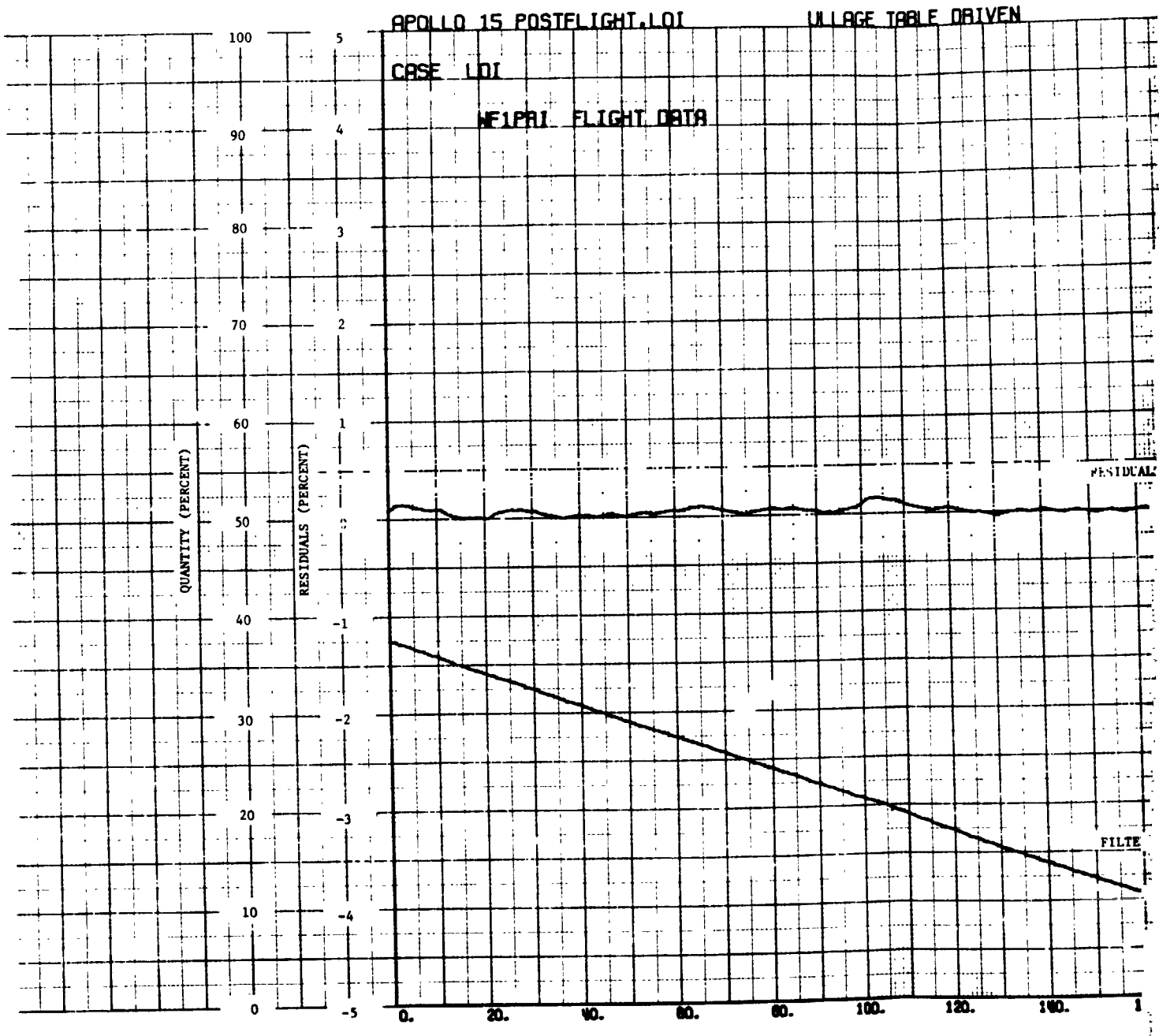

FOLDOUT FRAME

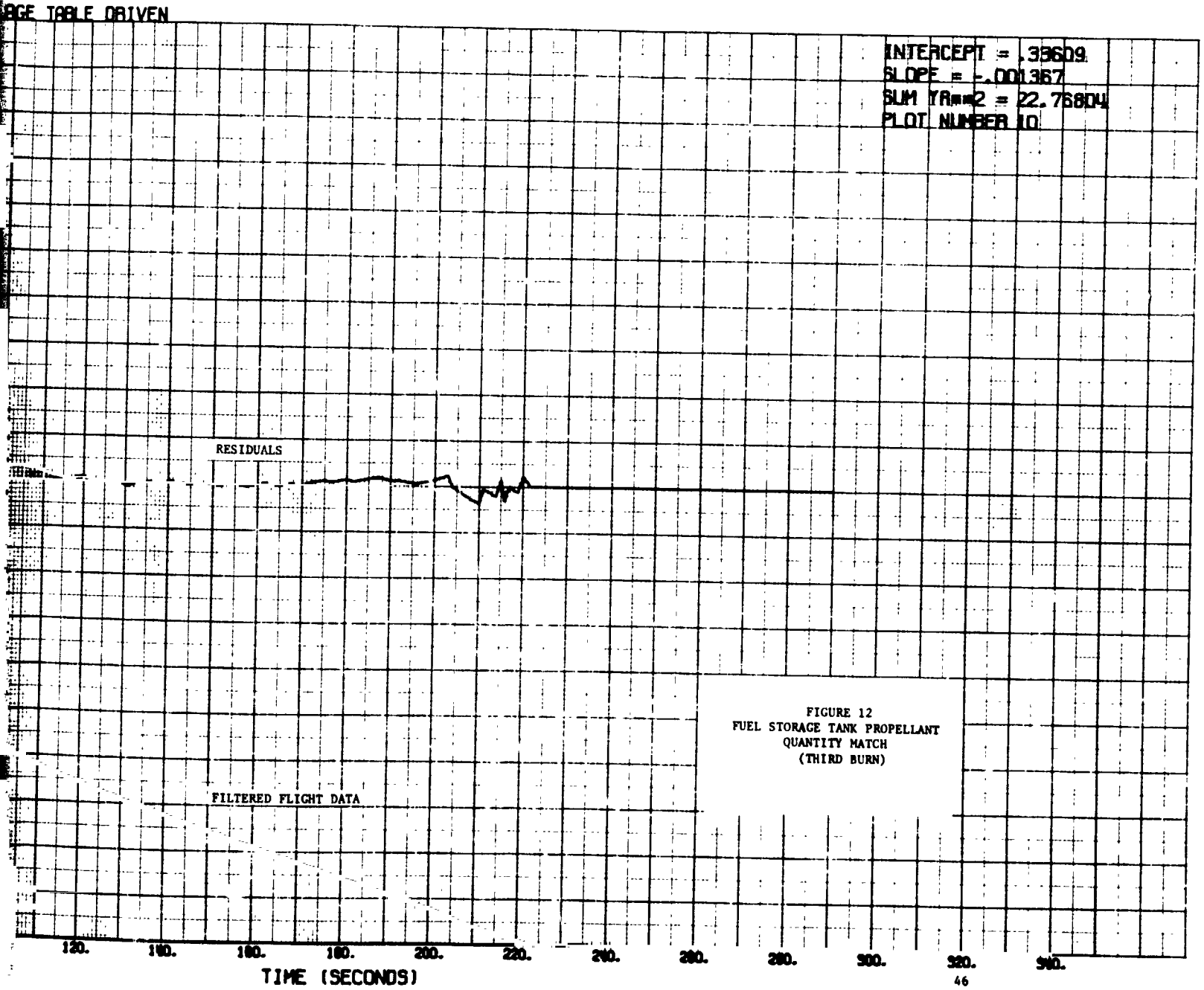

FIGURE 12
FUEL STORAGE TANK PROPELLANT
QUANTITY MATCH
(THIRD BURN)

FOLDOUT FRAME
2

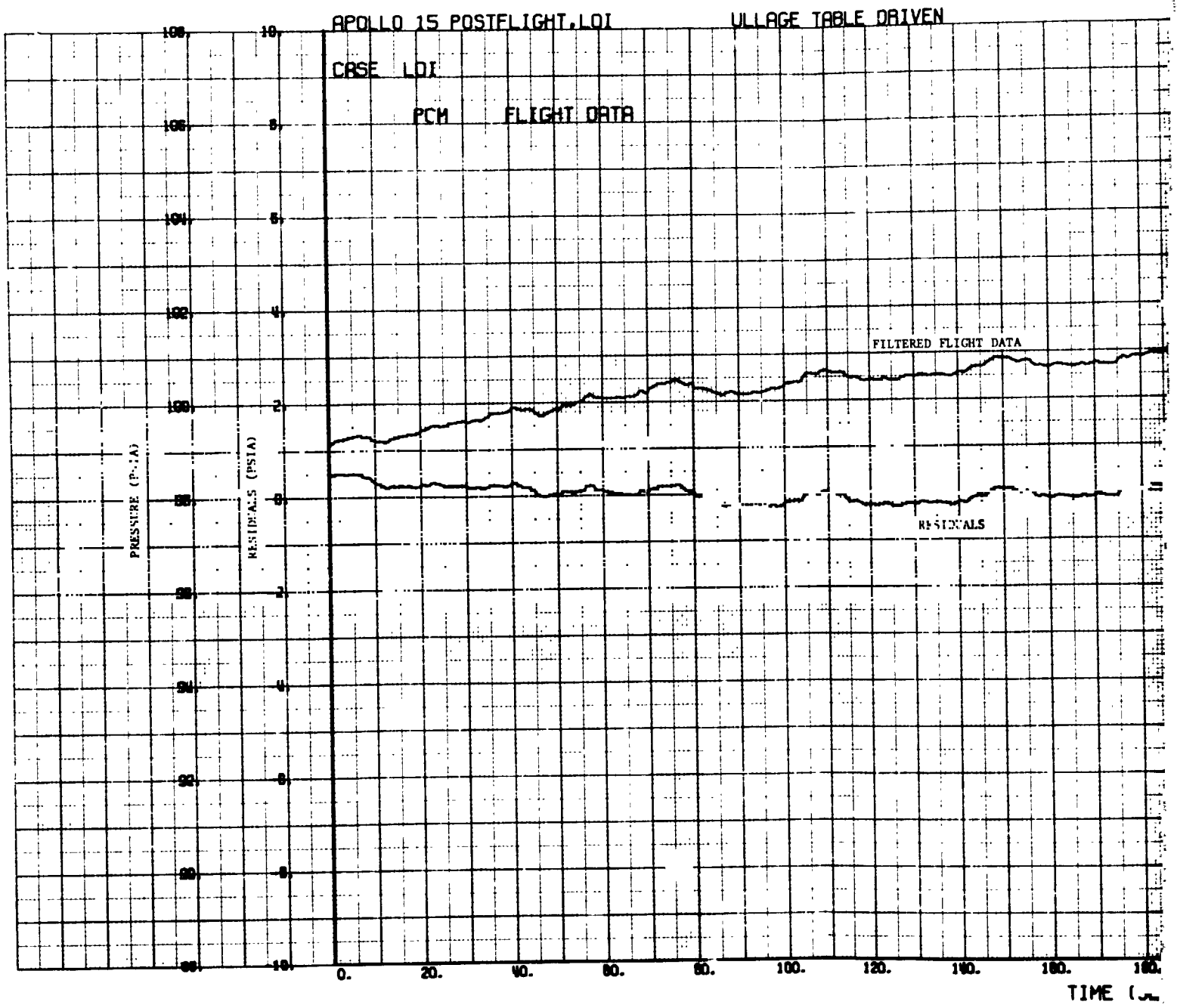

FOLDOUT FRAME

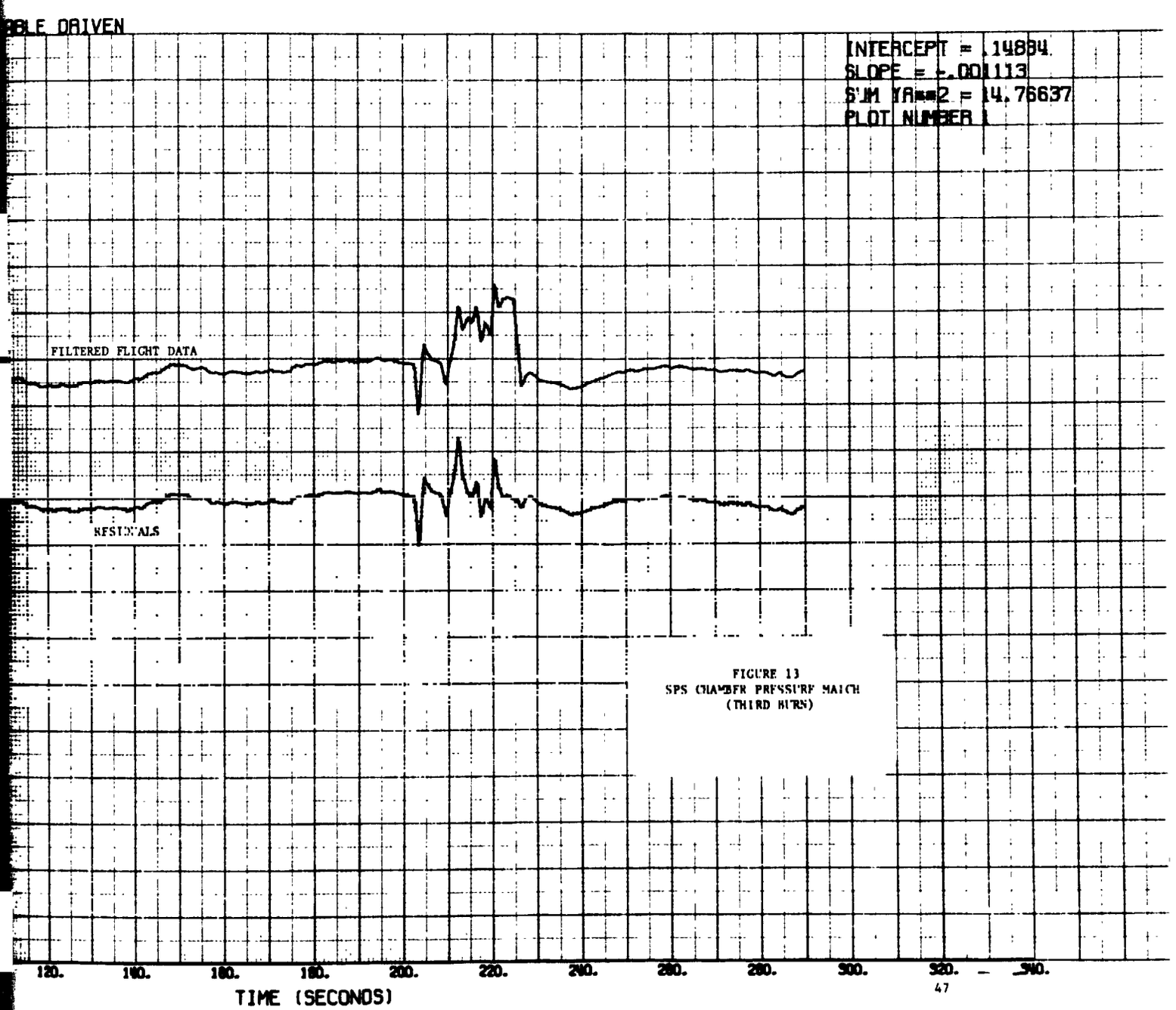

FIGURE 13
SPS CHAMBER PRESSURE MATCH
(THIRD BURN)

FOLDOUT FRAME

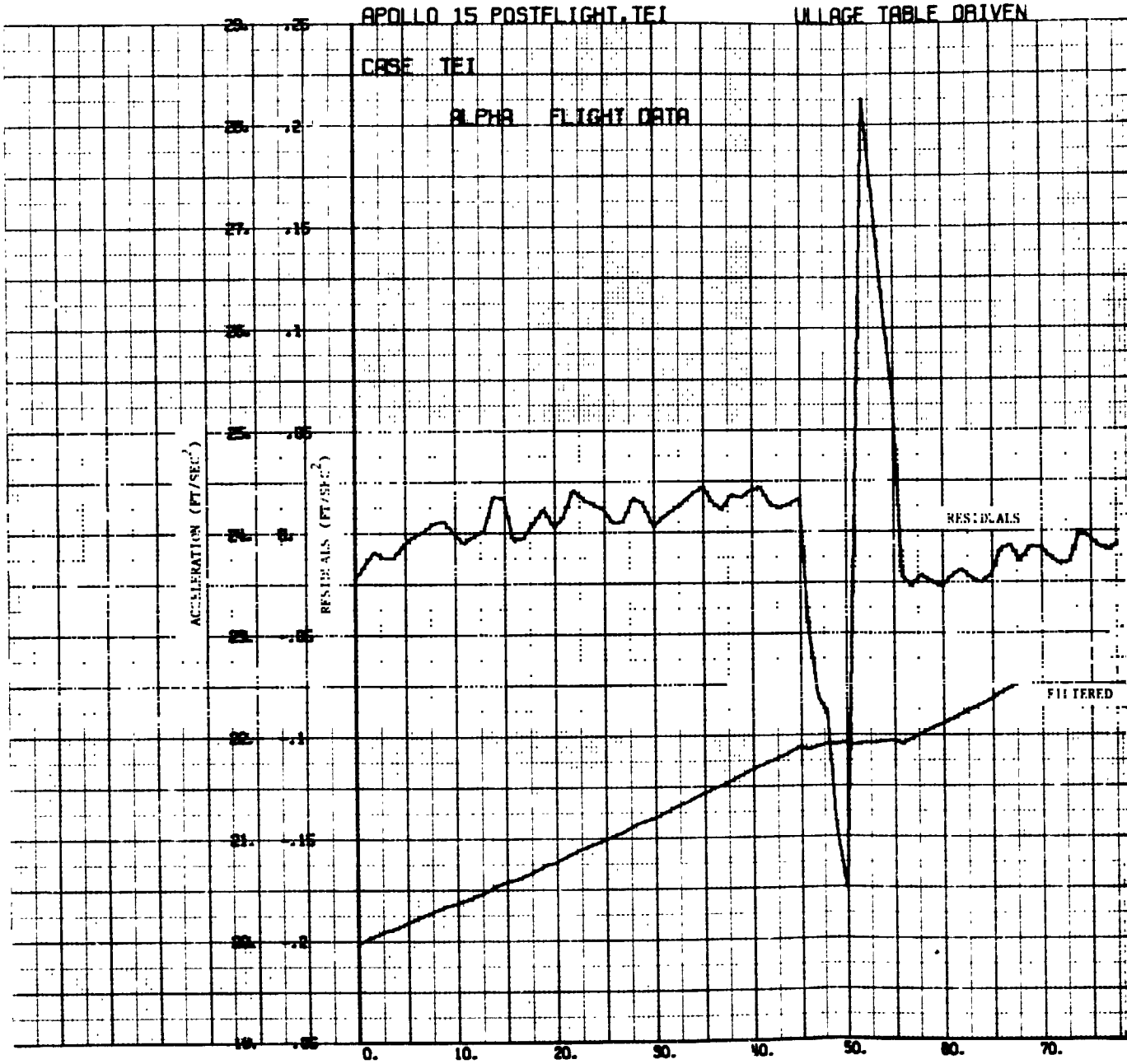

FOLDOUT FRAME

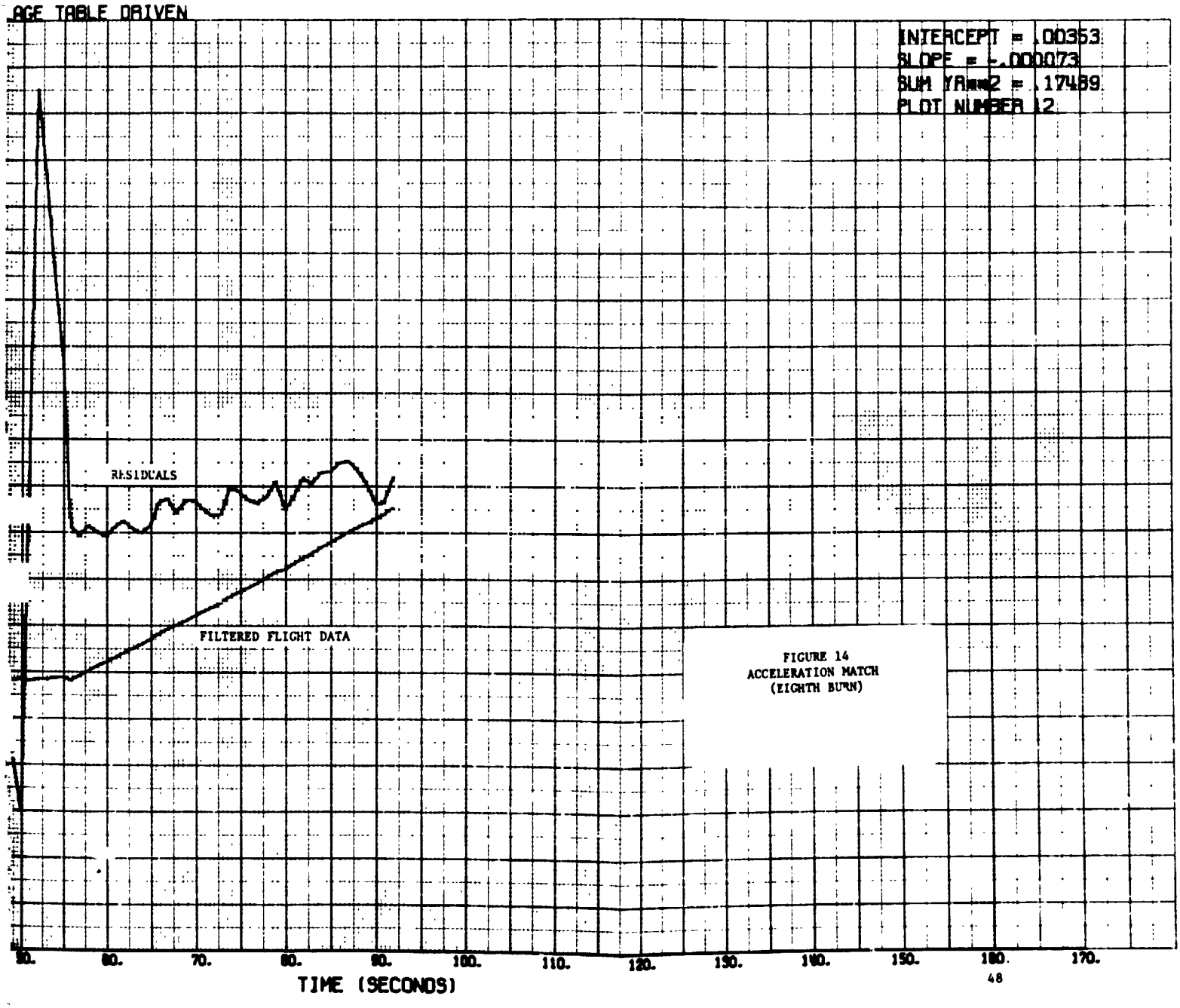

FIGURE 14
ACCELERATION MATCH
(EIGHTH BURN)

FOLDOUT FRAME

1

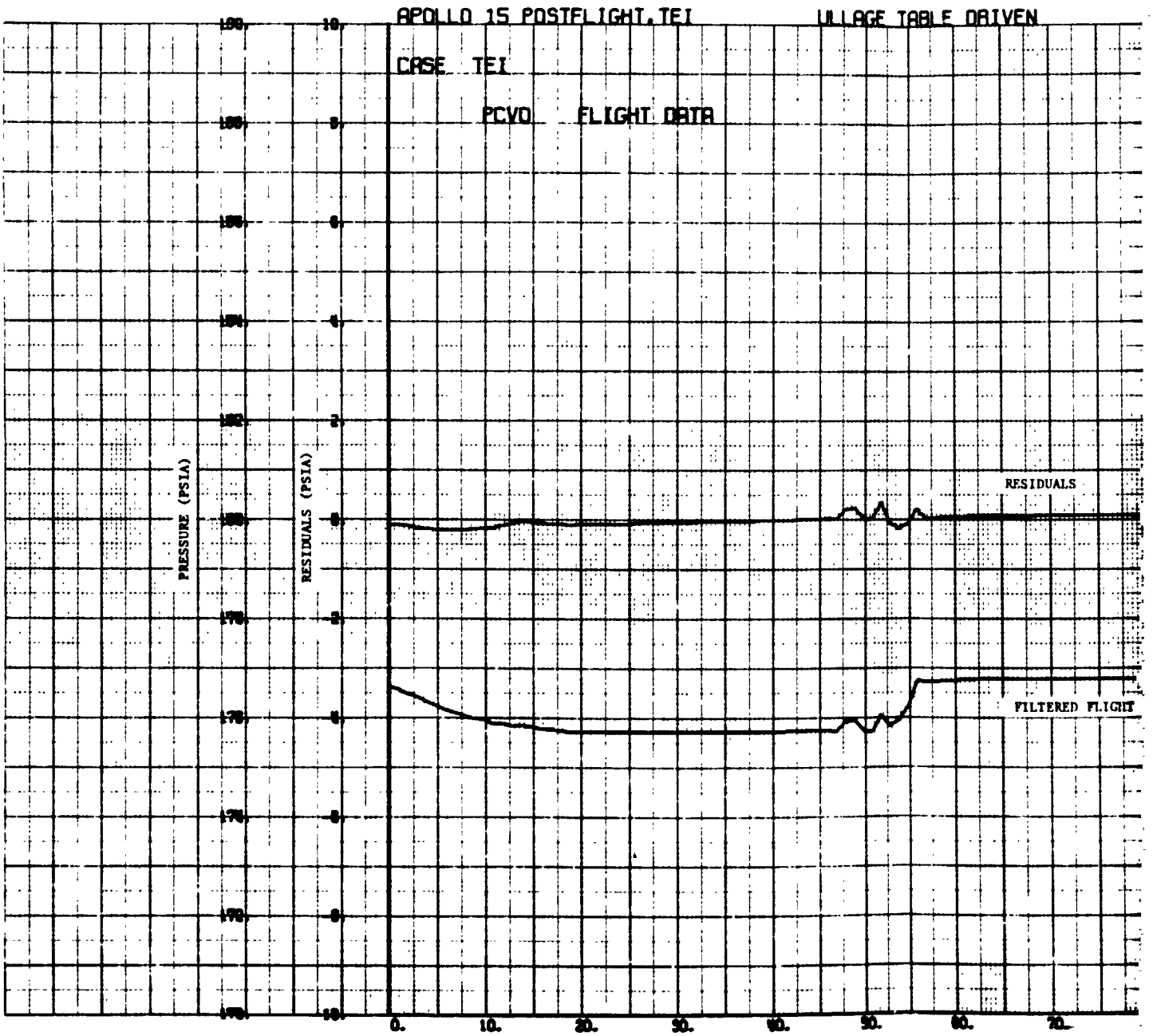

FOLDOUT FRAME

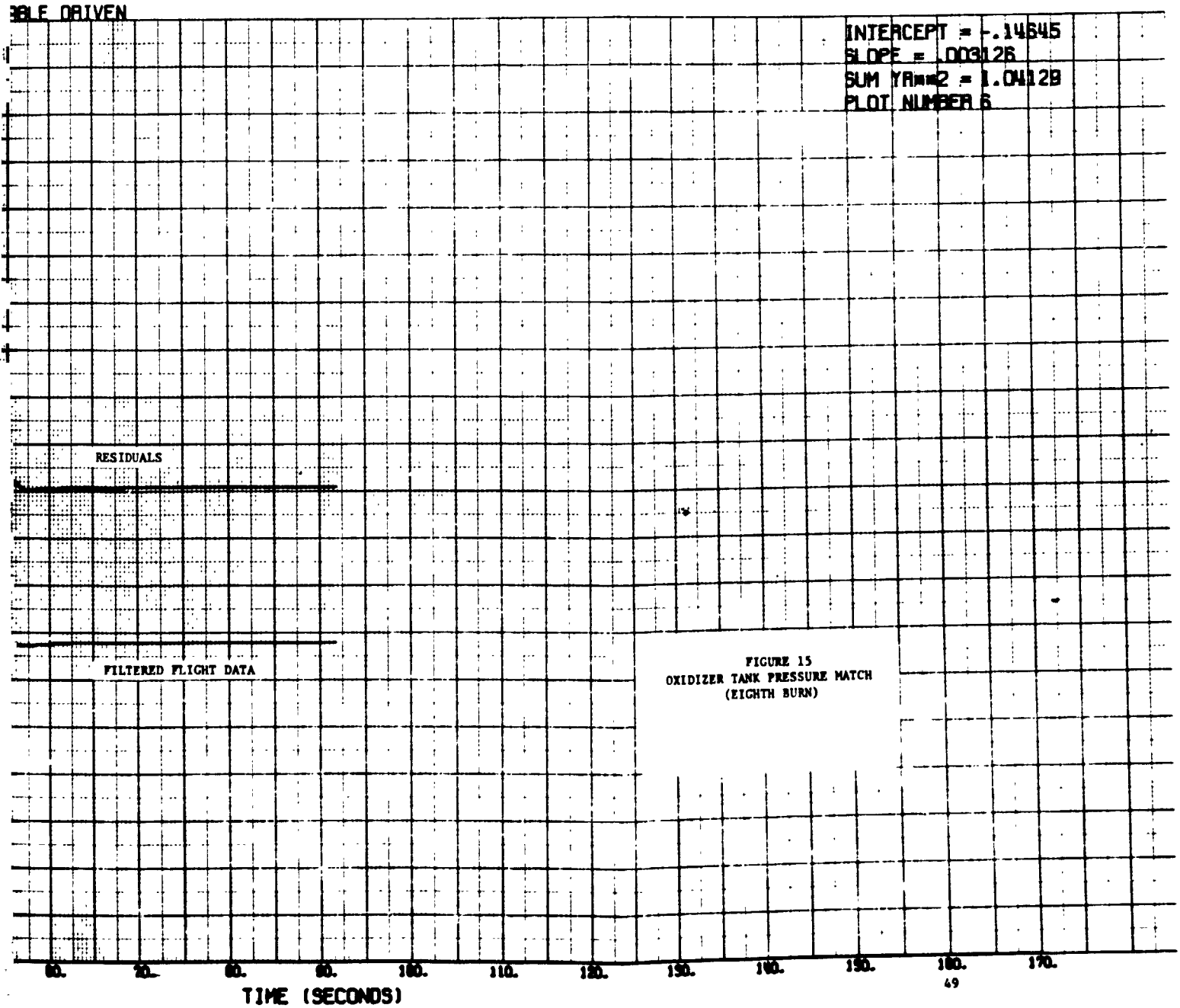

FIGURE 15
OXIDIZER TANK PRESSURE MATCH
(EIGHTH BURN)

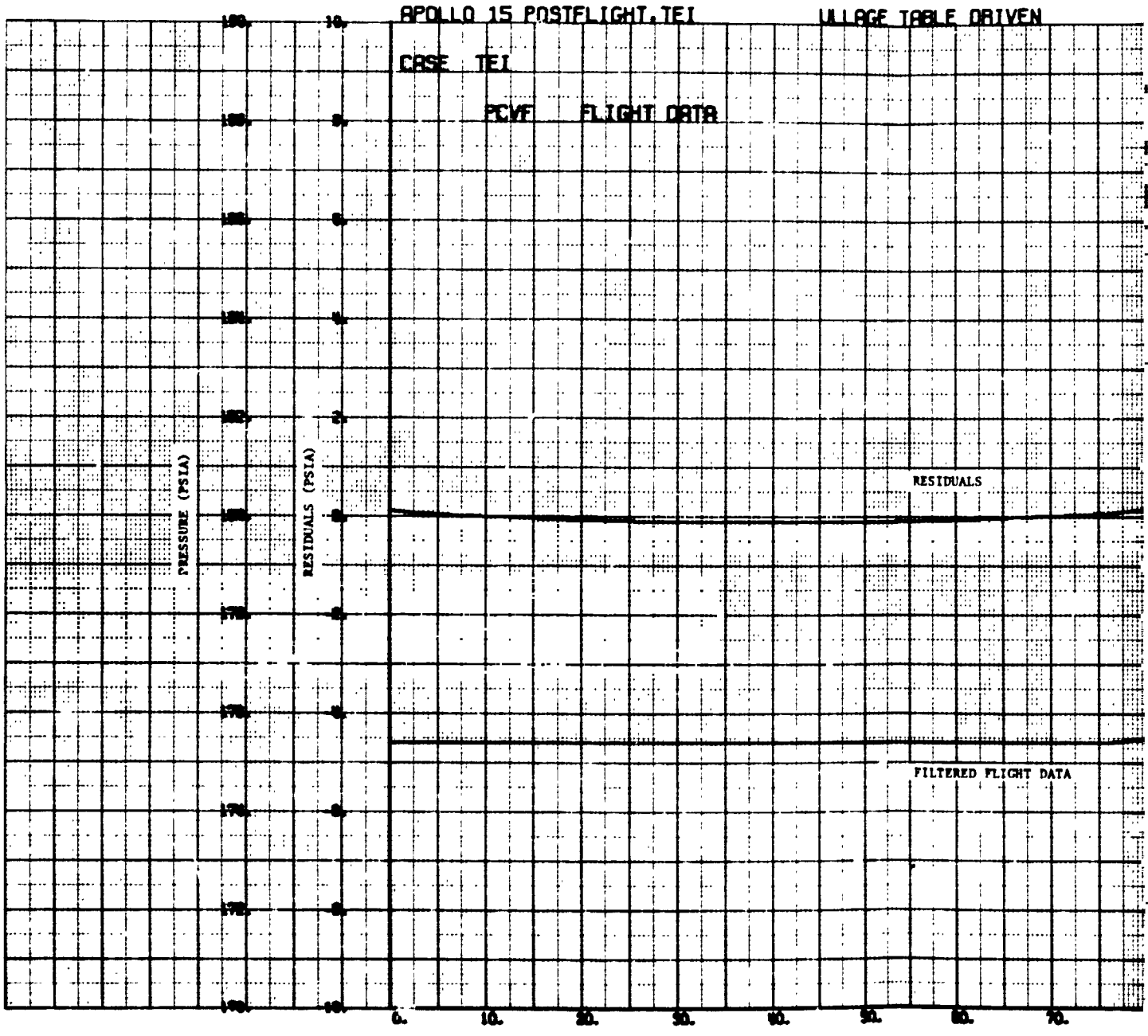

FOLDOUT FRAME

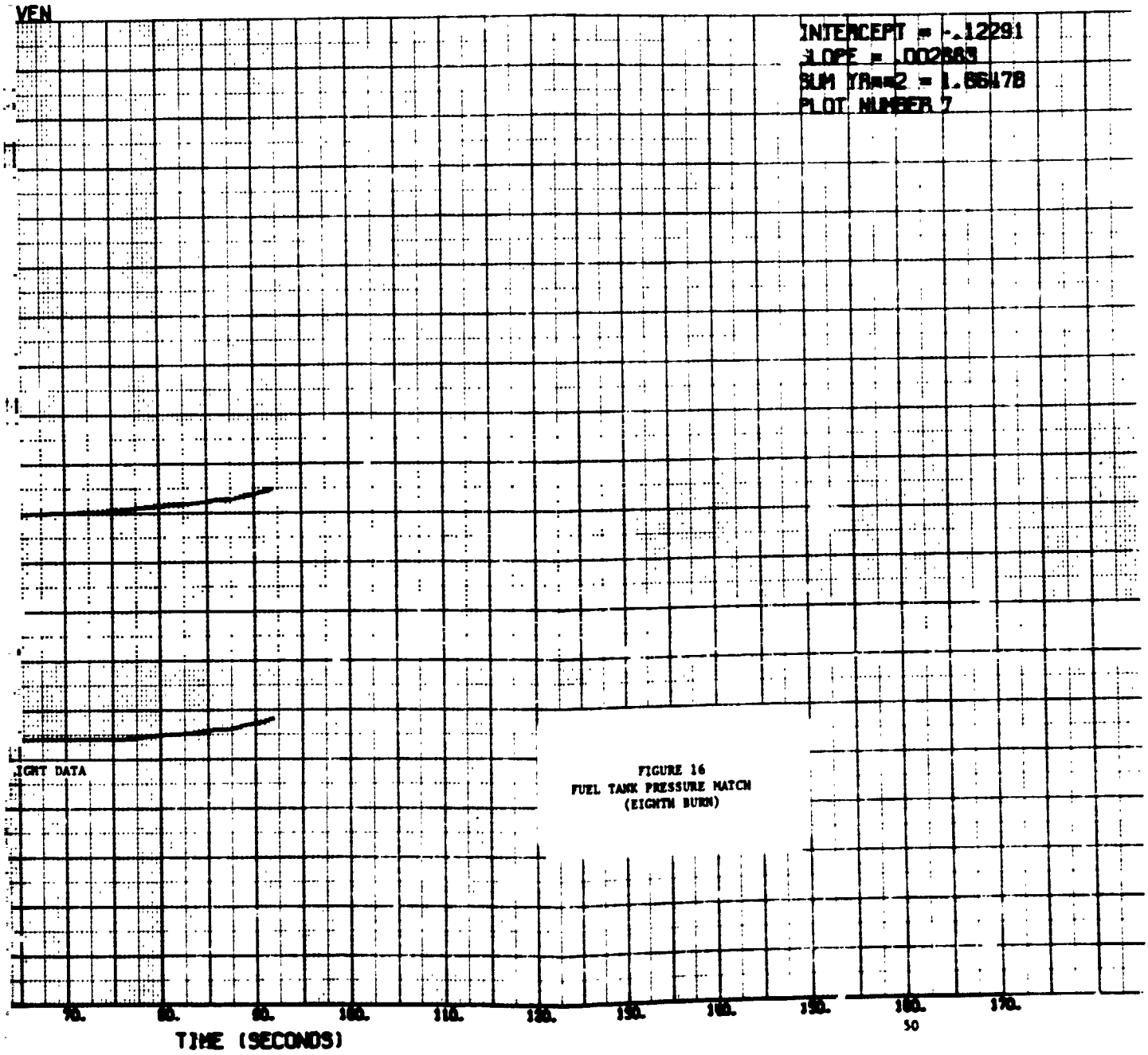

FIGURE 16
FUEL TANK PRESSURE MATCH
(EIGHTH BURN)

FOLDOUT FRAME

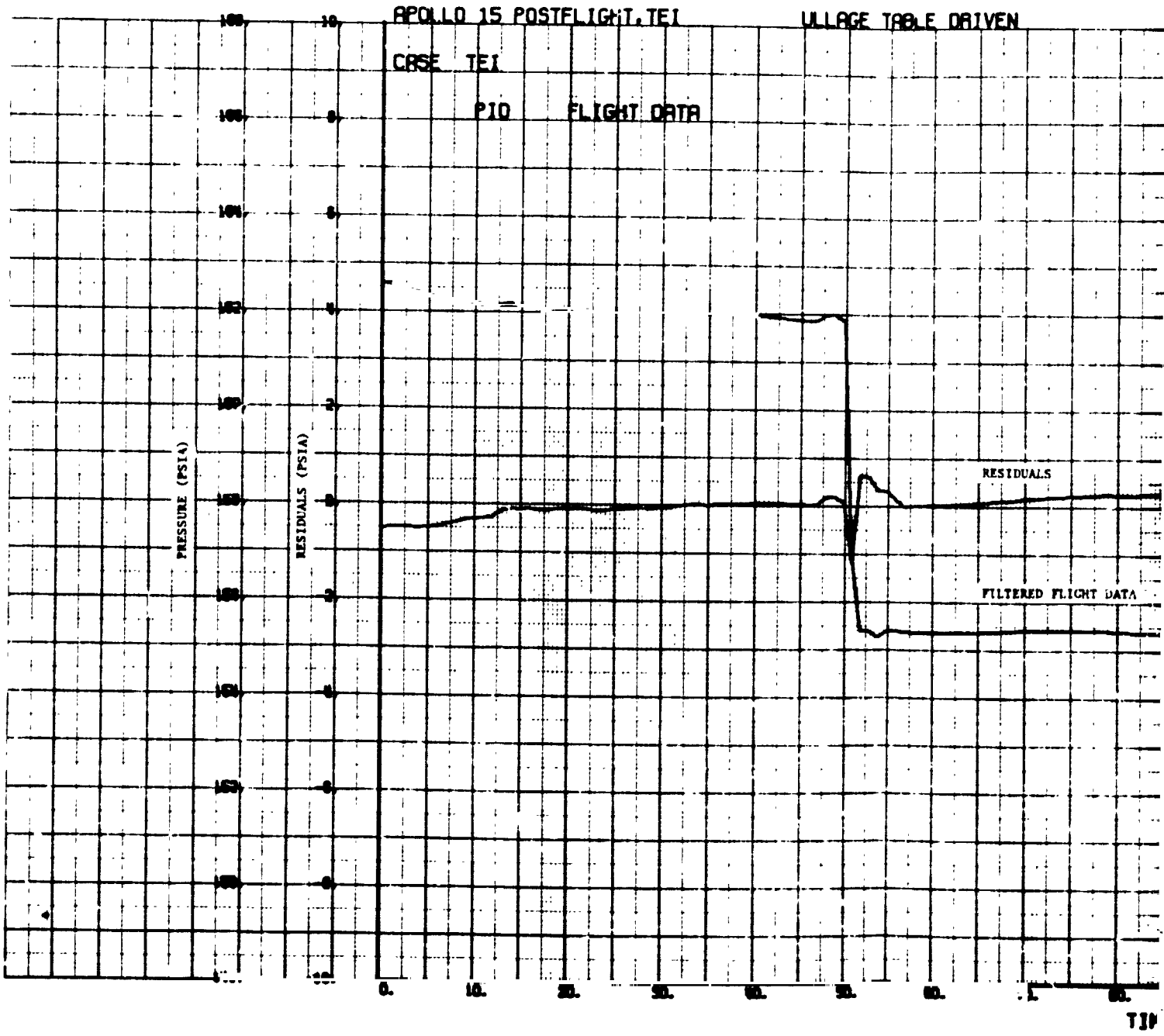

FOLDOUT FRAME

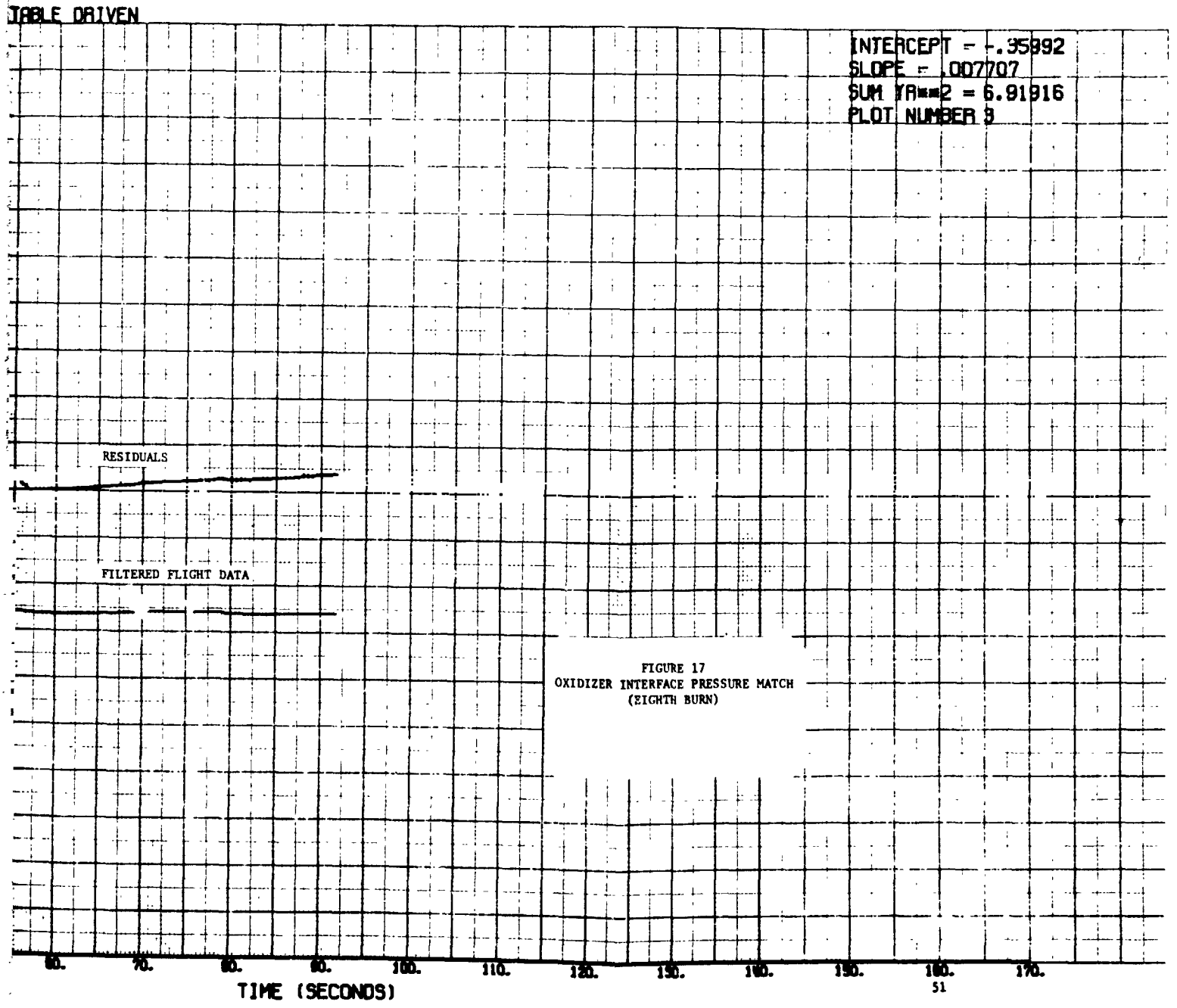

FIGURE 17
OXIDIZER INTERFACE PRESSURE MATCH
(EIGHTH BURN)

FOLDOUT FRA

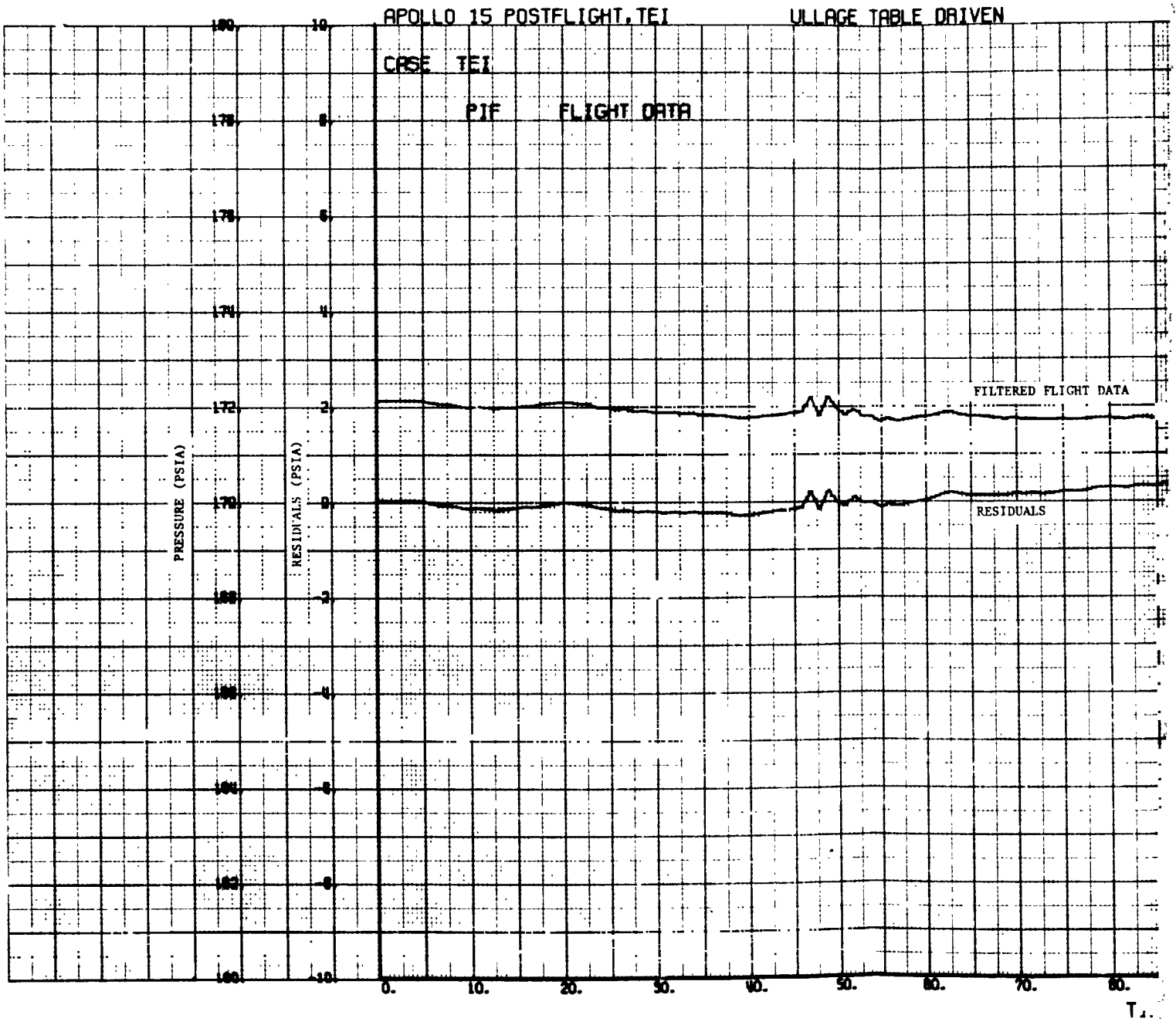

FOLDOUT FRAME

1

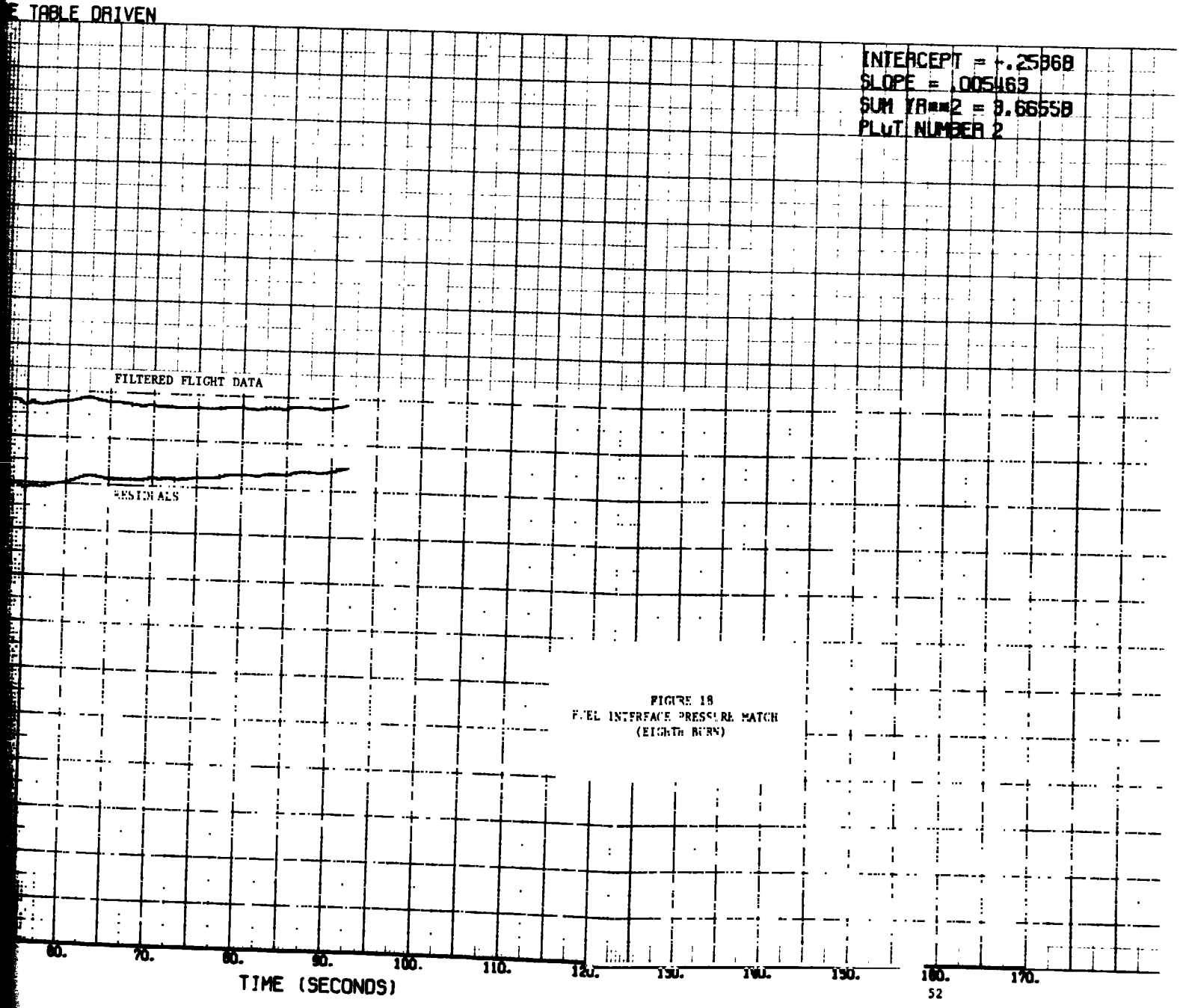

FIGURE 18
FUEL INTERFACE PRESSURE MATCH
(EIGHTH BURN)

FOLDOUT FRA...

2

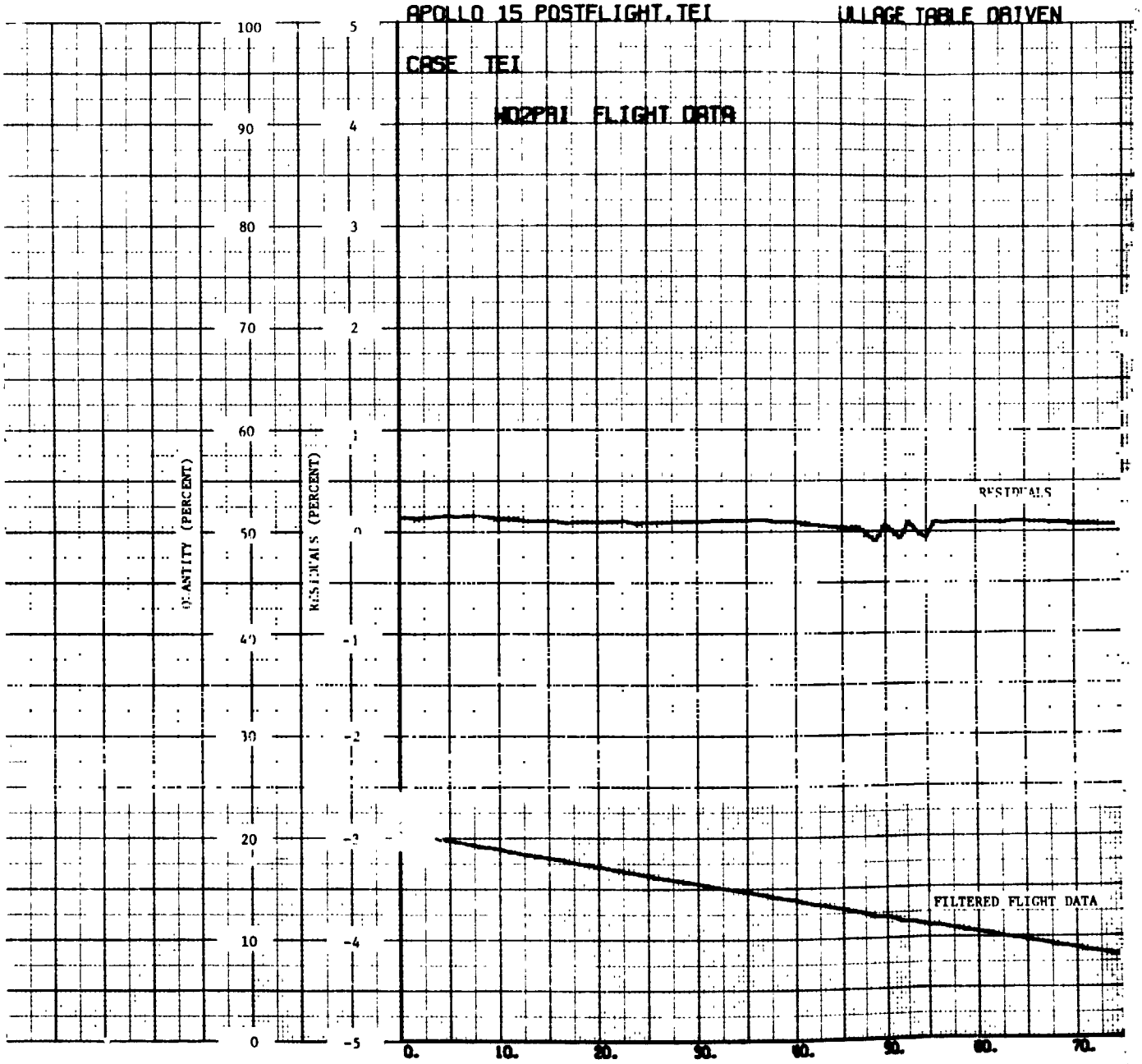

FOLDOUT FRAME

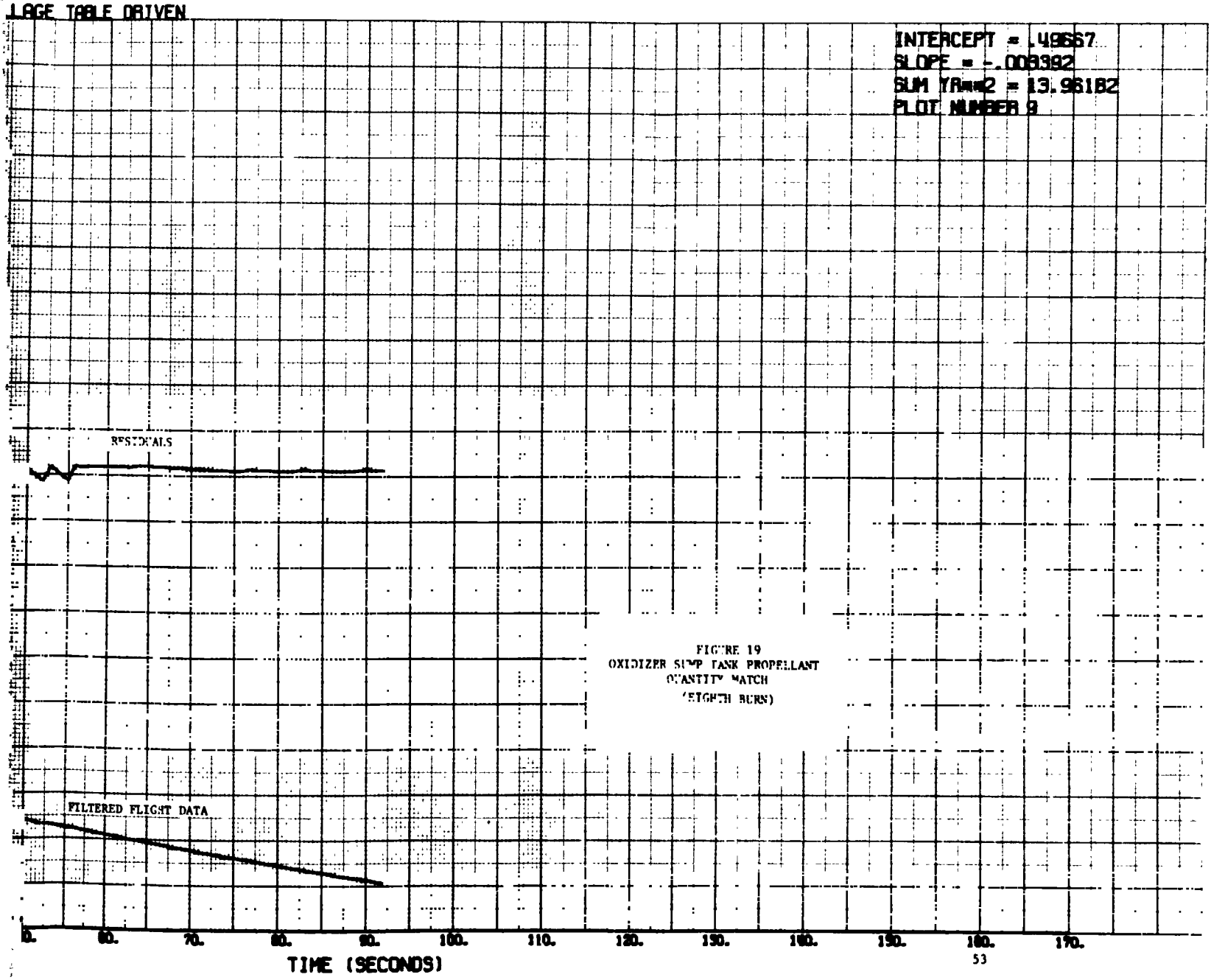

FIGURE 19
OXIDIZER SUMP TANK PROPELLANT
QUANTITY MATCH
(EIGHTH BURN)

FOLDOUT FRAME

1

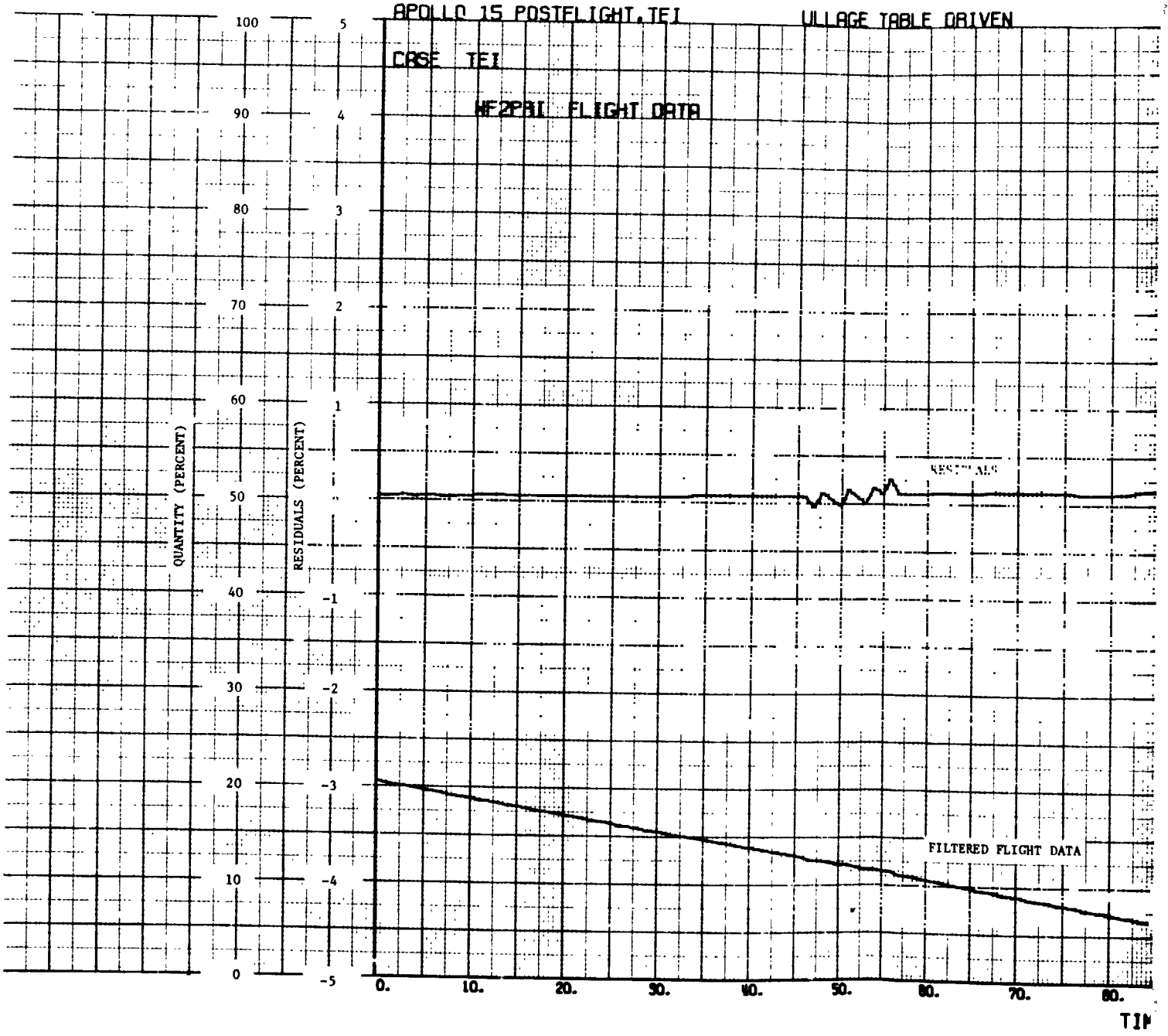

FOLDOUT FRAME

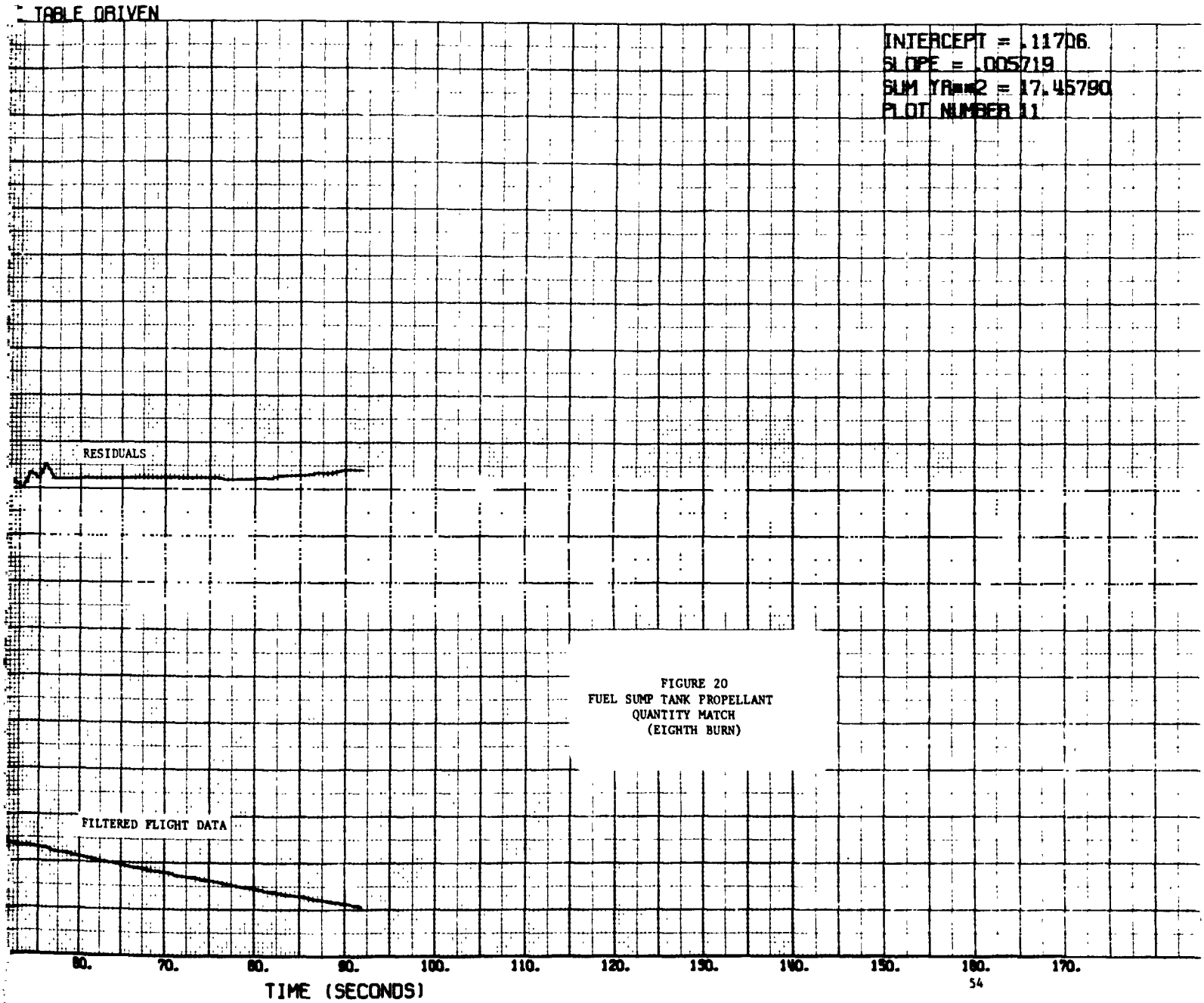

FIGURE 20
FUEL SUMP TANK PROPELLANT
QUANTITY MATCH
(EIGHTH BURN)

FOLDOUT FRAME

2

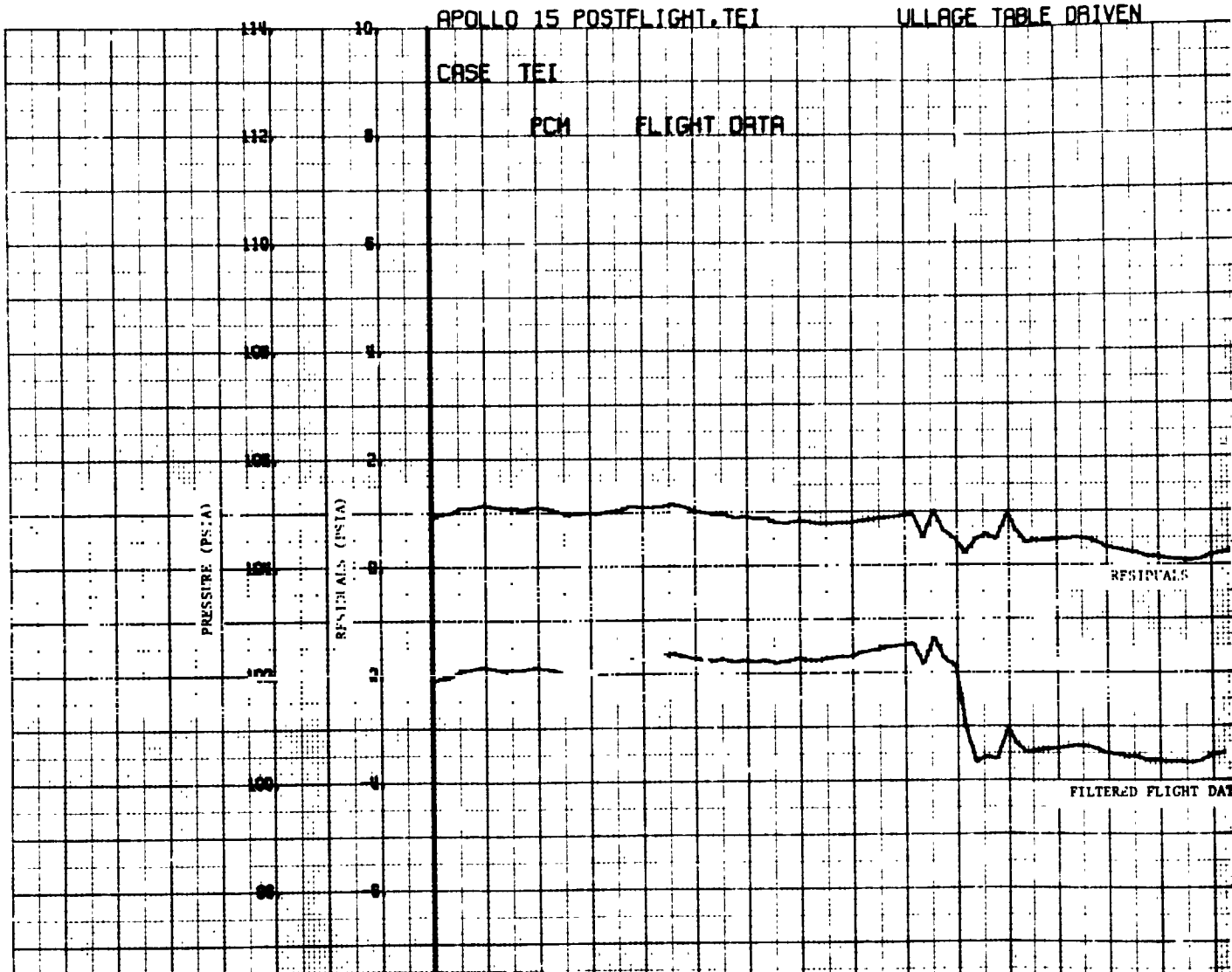

FOLDOUT FRAME

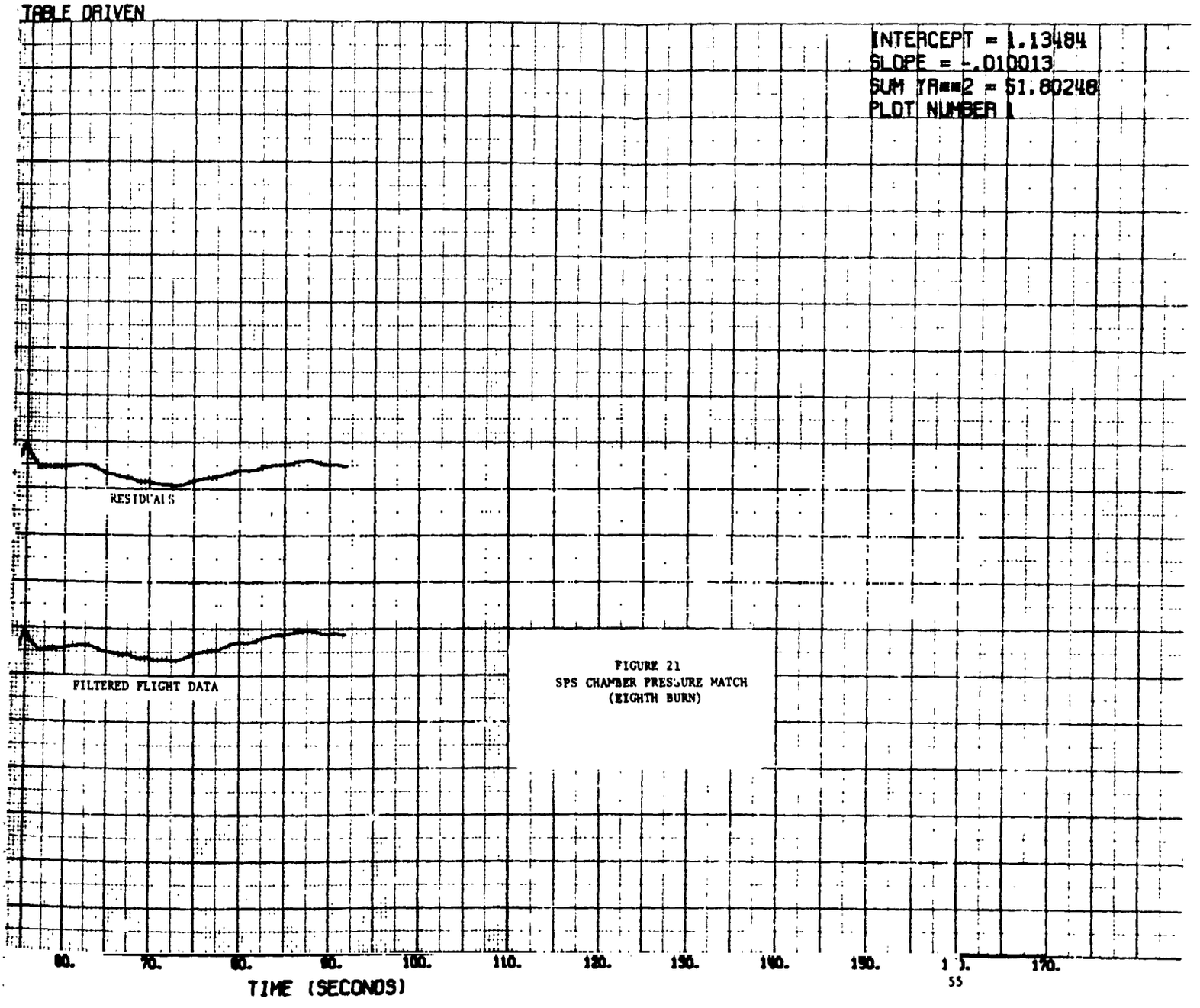

FIGURE 21
SPS CHAMBER PRESSURE MATCH
(EIGHTH BURN)

FOLDOUT FRAME

3

FIGURE 22

APOLLO 15

OXIDIZER INDICATED PROPELLANT UNBALANCE

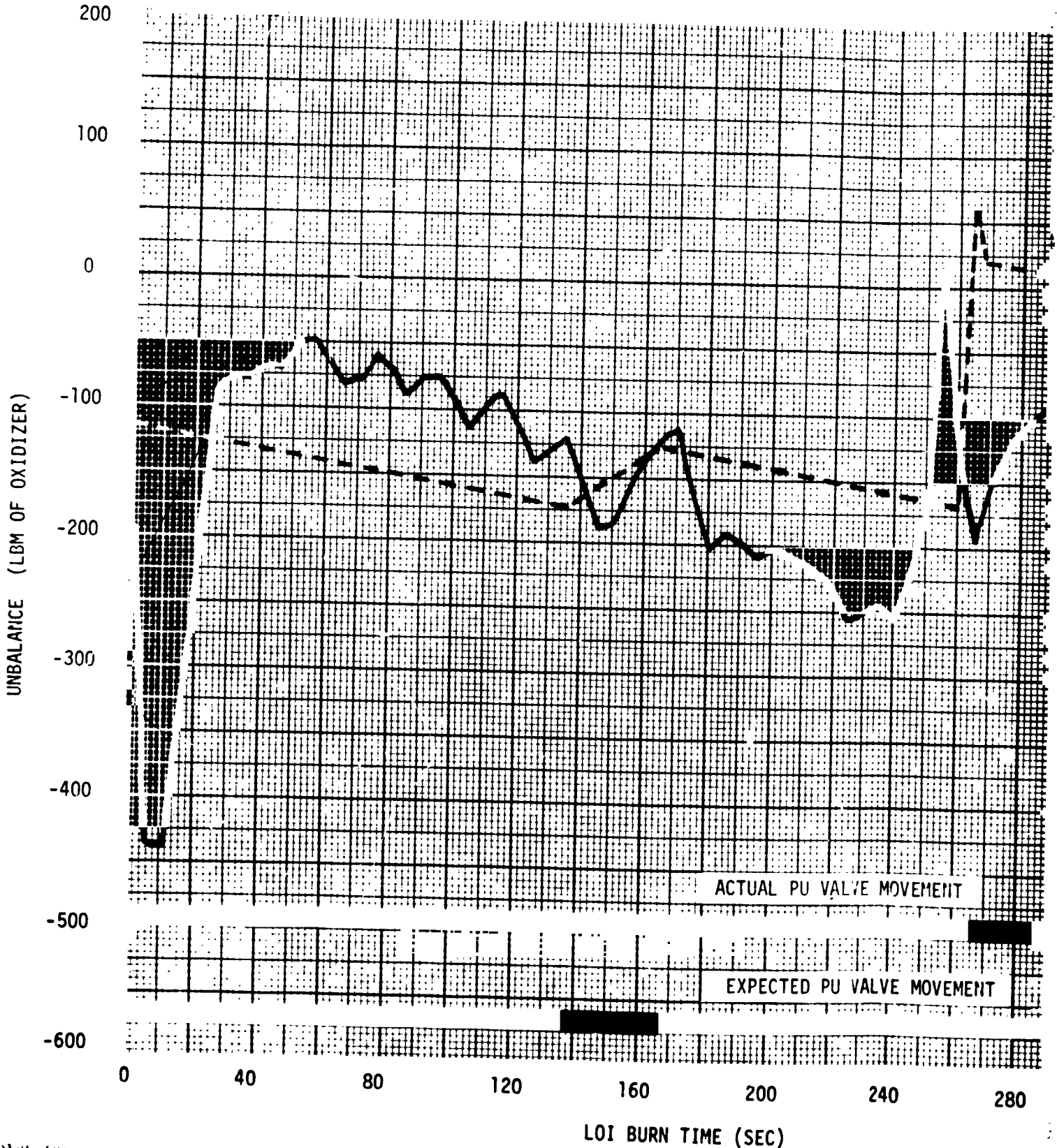

FOLDOUT FRAME

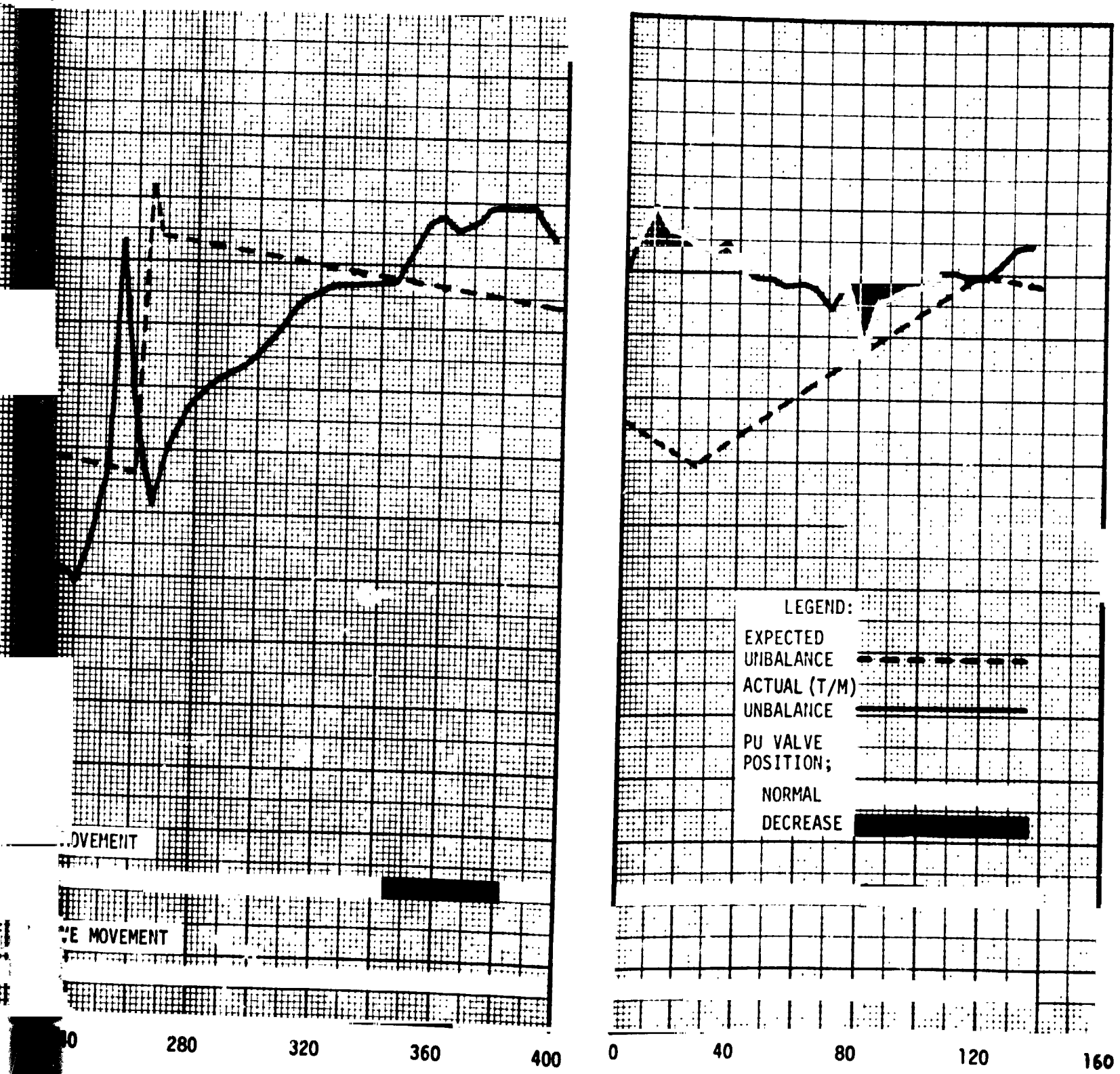

FOLDOUT FRA

5